U.S.N.A. --- Trident Scholar project report; no. 291 (2002)

ELECTRONIC RELIABILITY AND THE ENVIRONMENTAL THERMAL NEUTRON FLUX

by

Midshipman John David Dirk, Class of 2002
United States Naval Academy
Annapolis, Maryland

_____
(signature)

Certification of Advisors Approval

Professor Martin E. Nelson
Department of Mechanical Engineering

_____
(signature)

_____
(date)

Visiting Professor James Ziegler
Department of Physics

_____
(signature)

_____
(date)

Acceptance for the Trident Scholar Committee

Professor Joyce E. Shade
Deputy Director of Research & Scholarship

_____
(signature)

_____
(date)

USNA-1531-2

REPORT DOCUMENTATION PAGE

Form Approved
OMB No. 074-0188

1. AGENCY USE ONLY (Leave blank)	2. REPORT DATE	3. REPORT TYPE AND DATE COVERED
	6 May 2002	

4. TITLE AND SUBTITLE
Electronic reliability and the environmental thermal neutron flux

5. FUNDING NUMBERS

6. AUTHOR(S)
Dirk, John David

7. PERFORMING ORGANIZATION NAME(S) AND ADDRESS(ES)		8. PERFORMING ORGANIZATION REPORT NUMBER

9. SPONSORING/MONITORING AGENCY NAME(S) AND ADDRESS(ES)		10. SPONSORING/MONITORING AGENCY REPORT NUMBER
US Naval Academy Annapolis, MD 21402		**Trident Scholar project report no. 291 (2002)**

11. SUPPLEMENTARY NOTES

12a. DISTRIBUTION/AVAILABILITY STATEMENT	12b. DISTRIBUTION CODE
This document has been approved for public release; its distribution is UNLIMITED.	

13. ABSTRACT:

Boron, which is used in the manufacturing process of microelectronics, is highly sensitive to thermal neutrons. When ambient thermal neutrons originating from cosmic rays interact with the nucleus of boron, ionizing radiation is produced that can change the logic state of a cell on a microchip. This phenomenon is known as a Single Event Upset or Soft Error and is an important problem facing computer manufacturers. The goal of this project is to characterize the environmental thermal neutron flux with respect to electronic reliability by performing measurements of the thermal neutron flux in various locations at the United States Naval Academy and in surrounding sites.

The measurements were based on the use of two He3 gas-proportional counters, one detector was bare while the other was shrouded with boron-impregnated rubber that shielded it from thermal neutrons. The difference in the response between the two detectors yielded the thermal flux. The detectors were calibrated at the National Institute of Standards and Technology (NIST) and the Armed Forces Radiobiology Research Institute (AFRRI).

This project produced a portable, NIST traceable, accurately calibrated thermal neutron detection system. Measurements with that system showed a relatively constant thermal neutron flux from cosmic rays at sea level.

14. SUBJECT TERMS	15. NUMBER OF PAGES
thermal neutrons, single event upsets, helium-3, calibration, flux measurements, environmental	**95**
	16. PRICE CODE

17. SECURITY CLASSIFICATION OF REPORT	18. SECURITY CLASSIFICATION OF THIS PAGE	19. SECURITY CLASSIFICATION OF ABSTRACT	20. LIMITATION OF ABSTRACT

Abstract

Boron, which is used in the manufacturing process of microelectronics, is highly sensitive to thermal neutrons. When ambient thermal neutrons originating from cosmic rays interact with the nucleus of boron, ionizing radiation is produced that can change the logic state of a cell on a microchip. This phenomenon is known as a Single Event Upset or Soft Error and is an important problem facing computer manufacturers. The goal of this project is to characterize the environmental thermal neutron flux with respect to electronic reliability by performing measurements of the thermal neutron flux in various locations at the United States Naval Academy and in surrounding sites.

The measurements were based on the use of two He^3 gas-proportional counters, one detector was bare while the other was shrouded with boron-impregnated rubber that shielded it from thermal neutrons. The difference in the response between the two detectors yielded the thermal flux. The detectors were calibrated at the National Institute of Standards and Technology (NIST) and the Armed Forces Radiobiology Research Institute (AFRRI).

This project produced a portable, NIST traceable, accurately calibrated thermal neutron detection system. Measurements with that system showed a relatively constant thermal neutron flux from cosmic rays at sea level.

Keywords for Document Retrieval:
thermal neutrons
environmental
single event upsets
helium-3
calibration
flux measurements

Acknowledgments

This project would not have been successful without the assistance of many individuals. First the author would like to thank the International Business Machine Company of Yorktown, New York, which provided a grant to the U.S. Naval Academy to conduct this research. Second, technical assistance provided by Machinist's Mate First Class Kelly Delikat was invaluable to the project. Third the author thanks Alan Thompson of the National Institute for Standards and Technology for assistance in calibrating the detectors. Fourth, special thanks is given to Dr. Stephen Miller and John Nguyen of the Armed Forces Radiobiology Research Institute for their assistance in helping obtain a second calibration. Fifth, thanks to Drs. Wayne Newhauser and Uwe Titt of the Northeastern Proton Therapy Center, Boston, Massachusetts for graciously hosting the author in Boston in July of 2001. Sixth, the technical assistance given to the project by Drs. Noel Guardala and Gordon Riel at NSWC, Carderock is also appreciated. Finally, this project could not have been possible without the help and patience of the author's advisors Professor Martin Nelson and Visiting Professor James Ziegler of the U.S. Naval Academy.

Table of Contents

Table of Figures

List of Tables

Listing of Symbols and Abbreviations

Φ	Flux
$\Phi_{thermal}$	Thermal neutron flux
C	Calibration constant relating count-rate to flux
$\dot{N}$	Count-rate (counts / sec)
m	Mass
τ	Time constant of differentiation of integration
N	Avagadro's Number (6.022×10^{23} atoms / mole)
A_{eff}	Effective target area (cm^2)
N_{atoms}	Number of atoms
σ	Microscopic cross-section
Γ	Count-rate (counts / sec)
N_U	Number of uranium atoms
N_B	Number of boron atoms
R	Scaling ratio between two sources of different strengths
$I(x)$	Neutron flux at a given depth x
I_o	Incident neutron flux at depth = 0
λ	Single Event Upset rate
χ	Single Event Upset cross-section
AFRRI	Armed Forces Radiobiology Research Institute, Located in Bethesda, MD
BPSG	Boro-Phospho-Silicate Glass
DTRA	Defense Threat Reduction Agency
eV	electron-volt
GB	Gigabyte
HEU	Highly Enriched Uranium
HVPS	High Voltage Power Supply
IBM	International Business Machine Corporation
ICRP	International Commission on Radiological Protection
IT	Information Technology
MCA	Multi-channel Analyzer
MTF	Mean time to failure
NIMBIN	Nuclear Instrumentation Module Bin
NIST	National Institute of Standards and Technology (Formerly the National Bureau of Standards) Located in Gaithersburg, MD
NSWC	Naval Surface Warfare Center, Located in Carderock, MD
PC	Personal Computer
SEU	Single Event Upset
SHV	Safety, High Voltage type coaxial connectors
SRAM	Static Random Access Memory
TI	Texas Instruments
TNDS	Thermal Neutron Detection System, specifically the device developed by this project
TRIGA	Training, Research, Isotope, General Atomic Reactor
USB	Universal Serial Bus
USNA	United States Naval Academy, Located in Annapolis, MD

Chapter 1. Background

In the evolutionary march from the vacuum tube to the transistor, integrated circuit, and microprocessor, the electronics industry has sought to compress electronic devices to their smallest size. Additionally, the industry has sought to incorporate all the data processing functions of a circuit in a single integrated circuit chip. In doing so, and with an extensive understanding of the sources of electrical disturbances (from power supply noise to inter-logic radiation) they have been able to build systems designed to err less than once in every 10^{11} operations.[i]

The high hopes of computer designers for errorless systems are complicated, however, by cosmic rays from outer space. Cosmic rays incident upon the earth's atmosphere collide with atmospheric gases and produce a variety of particles that eventually reach the earth's surface. When these particles pass through a computer microchip, there is a small probability that it will interact with an atomic nucleus within the chip. Such a collision occasionally releases an electric pulse much larger than a regular logic pulse, which can be interpreted as an instruction and change the value of stored data or even incapacitate a microprocessor. [ii]

In military applications these sources of error are even more important. Nuclear weapons and propulsion reactors produce radiation similar to that from outer space. Aircraft, which fly at high altitudes, are subject to much higher (as much as 300 times higher) incidence of cosmic rays. In combat systems the possibility of a "soft error" rendering an electronic system unusable is a serious concern. Ensign Justin Sarlese (USNA '00) modeled the aircraft problem as part of the Trident Scholar program in 1999-2000. [iii]

Although the electronics industry is aware of the problems cosmic rays cause, they are unable to fully address them because the random and rare induced bursts of charge are so large that they overwhelm normal noise tolerances. Further, the nature of the problem evolves with the natural evolution of integrated circuit design. This study concerns a new version of this old problem. This new problem began occurring in 1998 and has recently has become important enough that it is the subject of articles in Computer World, Forbes and other IT news media (see excerpts Figure 1-1). These reports are somewhat confused because the press has difficulty distinguishing problems due to alpha particles, cosmic rays and other ambient radiation. The alpha particles these articles refer to are from previous problems that the semiconductor industry experienced from radiation effects on their chips. These problems came from contamination of the semiconductor factories with trace amounts of radioactivity, which led to chips with enough radioactivity to cause serious performance problems including device failure. The possibility that environmental radiation could become a reliability problem has been known for at least a decade. As circuits have become increasingly small and have come to operate at lower and lower voltages the interaction has become a practical problem.[iv]

The cause of the problem noted in these press articles arose from the introduction of a thick layer of boro-phospho-silicate glass (BPSG) as the method of smoothing the chip surface before the many layers of metallurgy are applied.[v] This new technology was developed in the early 1990's and solved one of the most costly and difficult problems in the semiconductor industry. In the short period of about four years it was adopted by many manufacturers (it was excluded purposely from Texas Instruments because they realized the potential problem it might pose[vi-ix]). BPSG contains about 9% boron, and 20% of this boron

consists of the isotope B^{10}. This isotope is extremely sensitive to the last vestiges of the cosmic ray shower: thermal neutrons. These neutrons have a relatively long lifetime in the terrestrial environment because they have a high probability of interaction only with rare atoms like cadmium, uranium or boron-10 and a low probability of interaction with common atoms such as hydrogen, oxygen, and carbon. When a thermal neutron encounters an atom of B^{10}, a nuclear reaction occurs which releases enough energy to overpower any nearby circuit elements, causing a computer error.

Very little is known about thermal neutrons in the terrestrial environment. Before 1995, only two scientific papers mentioned them. A theoretical paper in 1978 calculated that their density might vary by more than 100x from place to place because of the presence of absorbers like water (less than 1m of water can absorb 99% of local thermal neutrons).[x] A second paper measured the flux of thermal neutrons at about 100/cm^2-hour.[xi] Texas Instruments has recently published three papers on this subject, and their measurements indicated fluxes ranging from 10 to 67 neutrons/cm^2-hour.[vi,xii] They did not comment on this remarkable variation and are no longer involved in this work. Work at IBM has indicated a measured thermal neutron flux of about 2/cm^2-hour.[xiii]

There is no way to predict the error rate of modern electronics unless the thermal neutron environment is understood. The sensitivity of chips to thermal neutrons can be measured, but without understanding the local flux of neutrons the chip upset rate can not be predicted.

This research project sought to measure the thermal neutron flux in the environment and identify if any large (50-100x) variation existed in it. Thermal Neutrons are those who

are in thermal equilibrium with the atoms that compose the surrounding material. At room temperature the most probable value for their energy is .025 eV. For the purposes of this report, all neutrons below 1 eV will be considered thermal or slow neutrons. Neutrons above 1 eV will referred to as fast neutrons. The report will first discuss detection technology in chapter 2, both that considered and the technology actually used. Chapter 3 describes in detail the construction and operation of the U.S. Naval Academy Thermal Neutron Detection System (USNA TNDS) and discusses briefly other systems developed in parallel with the TNDS. Chapter 4 describes the successful calibration efforts at both the National Institute of Standards and Technology (NIST), Gaithersburg, Maryland, formerly the National Bureau of Standards, and the Armed Forces Radiobiology Research Institute, Bethesda, Maryland. The field measurement efforts are discussed in chapter five. Several thermal flux attenuation experiments are detailed in chapter five as well. Finally conclusions and recommendations are given in chapter 6.

Press Accounts of Recent Problems of Cosmic Rays and Computers

"Sun Releases First Computers based on New Chip"
***Server News*, 26 September, 2000.**

Quote from article: 'Sun Microsystems has been having problems with its cache memory.... and has stopped buying components from one of its two SRAM suppliers.'

"Sun Microsystems tries to hush dissatisfaction over memory woes"
***Computer World*, 18 September, 2000.**

Quote from article: 'Sun admits to a memory problem in its newest servers. Under certain conditions it triggers system failures and frequent server reboots at dozens of customer locations.'

"More Users Slam Sun for Memory Issue",
***Computer World*, 4 September, 2000.**

Quote from article: 'Sun engineers have come out to our location repeatedly to fix our servers. The replace everything but the frame. They don't seem to know how to fix the problem.'

"Sun Microsystems' Servers have been Crashing for more than a Year and Sun hasn't yet Fixed It",
***Forbes*, 13 November, 2000.**

Quote from article: 'Sun says that it has finally figured out what's wrong. It is an odd problem involving stray cosmic rays and its memory chips... The faulty chips are easily distupted by stray radiation, alpha particles or cosmic rays, which can turn a single bit 0 into a 1. When the computer detects an error, it automatically shuts down (crashes).'

"Sun Under Fire for Crashes"
***Information Technology News*, 9 Nov. 2000.**

Quote from article: 'The cause of the problem is a mystery. A leading contender: cosmic rays, specifically alpha particles, which collide with molecules in the server's memory and change the value of a single bit of memory, enough to crash the server. Although that theory sounds 'X-Files'-ish, there is scientific precedent, said analyst Paul McGuckin of the Gartner Group.

"Radiation - Induced Computer Malfunctions"
***International Chemistry*, 22 May, 2000.**

Quote from article: 'Although computer glitches will result from catastrophic releases of radiation (such as nuclear warfare), naturally occurring radiation has thus far posed the greater threat to the computer user. And, although the average user may naively blame software alone for errors and crashes, the guilt must be shared with natural, ever-present, environmental radiation.'

Figure 1-1 Press accounts of recent radiation related computer problems

[i] J. Ziegler, USNA, private communication.

[ii] See the extensive review of the effects of cosmic rays and radiation on modern electronics in the IBM Journal of Research and Development, vol. **40**, 1996.

[iii] J. A. Sarlese, "Development of a Semi-Empirical Model for SEUs in Modern DRAMs," Trident Scholar Project Report; no. 277, U.S. Naval Academy, May 2000.

[iv] Baumann, R.C., Texas Instruments Co., private communication.

[v] S. Wolf and R. N. Tauber, "*Silicon Processing for the VLSI Era*", Lattice Press, 186 (1986).

[vi] R. Baumann, T. Hossain, E. Smith, S. Murata and H. Kitagawa, "Boron as a primary source of radiation in high density DRAMs, *IEEE 33rd Annual Intnl Reliability Physics Proc.*, 297-302 (1995).

[vii] R. C. Baumann, T. Z. Hossain, S. Murata, H. Kitagawa, "Boron Compounds as a Dominant Source of Alpha Particles in Semiconductor Devices." IEEE Proc. IRPS, p. 297, 1995. .

[viii] R. C. Baumann and E. B. Smith, "Neutron-induced ^{10}B fission as a major source of soft errors in high density SRAMs," *Microelectronics Reliability*, vol. **41**, no. 2, p.211, 2001.

[ix] R. C. Baumann and E. B. Smith, "Neutron-Induced Boron Fission as a Major Source of Soft Errors in Deep Submicron SRAM Devices," IEEE Proc. IRPS, p. 297, 2000.

[x] K. O'Brien, H. A. Sandmeier, G. E. Hansen and J. E. Campbell, J. Geophys. Res., **83**, 114 (1978).

[xi] G. Heusser, "The Background Components of Germanium Low-Level Spectrometers," Nucl. Inst. and Methods, **B17**, 418-422 (1986).

[xii] R. Baumann, "Soft Error Characterization and Modeling Methodologies at Texas Instruments," Semiconductor Research Council 4th Topical Conf. On Reliability, SemaTech CD-ROM 0043-3283 (2000).

[xiii] T. Zabel, IBM-Research, private communication.

Chapter 2. Detectors

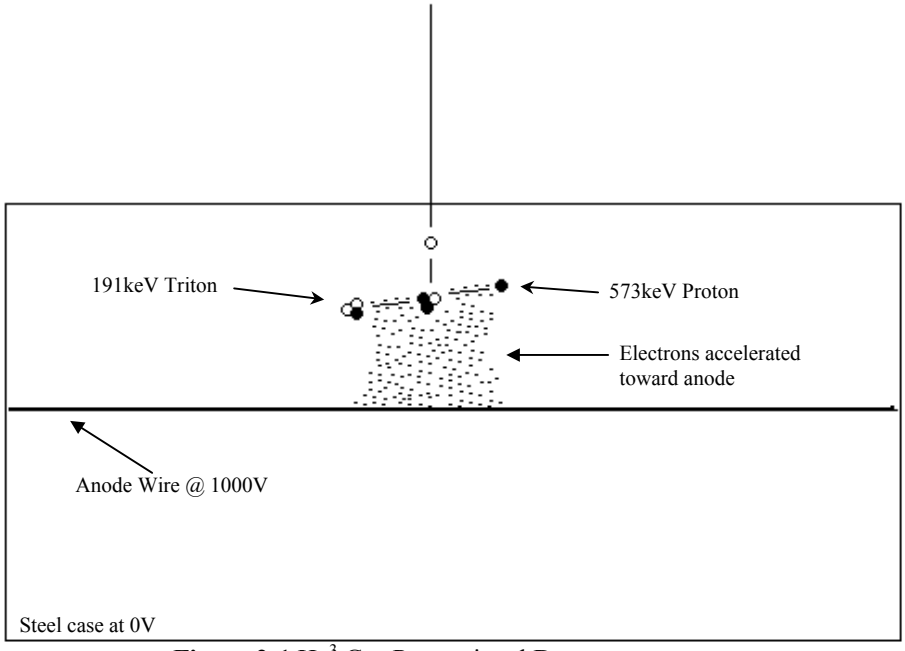

Figure 2-1 He^3 Gas Proportional Detector

This chapter discusses the basic principles behind neutron detection equipment with an emphasis on detection protocols considered or evaluated for this project. Because they are uncharged particles, neutrons are difficult to detect. Still more difficult is separating the thermal, or slow neutrons, from the total neutron flux. The two most common approaches to neutron detection utilize either gas-proportional counters or scintillator based detectors.

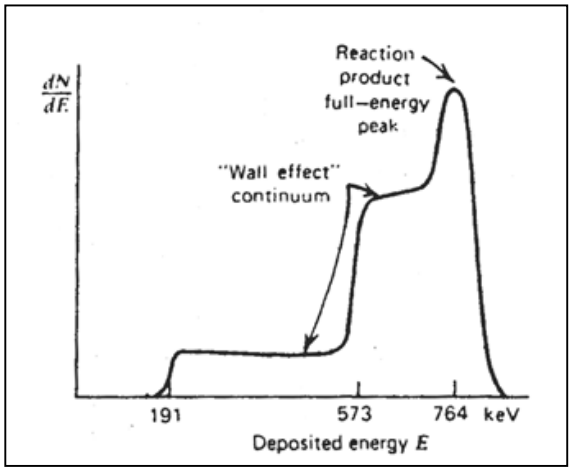

Figure 2-2 Expected pulse height spectrum from a small ^3He tube in which the wall effect is significant (from Knoll).[12]

The gas-proportional counter is a steel tube filled with a neutron sensitive gas such as He^3 or BF_3 (see figure 2-1). The tubes

are pressurized to several atmospheres to increase the density of the sensitive element. A thin wire runs the length of the tube and is insulated from the tube's outer case. A bias of several hundred volts to several kilovolts is applied between the wire and the outer case. The wire acts as an anode. When an incident neutron collides with one of the gas molecules, He^3 for example, the molecule may undergo a nuclear reaction, such as:

$$^0n^1 + He^3 \rightarrow H^3 + {}^1p^0 + 764keV$$

The energy released by the reaction is in the form of the kinetic energy of the recoil particles, the proton and triton. As the charged particles move through the detector gas they ionize the gas molecules. The liberated electrons are accelerated towards the anode wire by

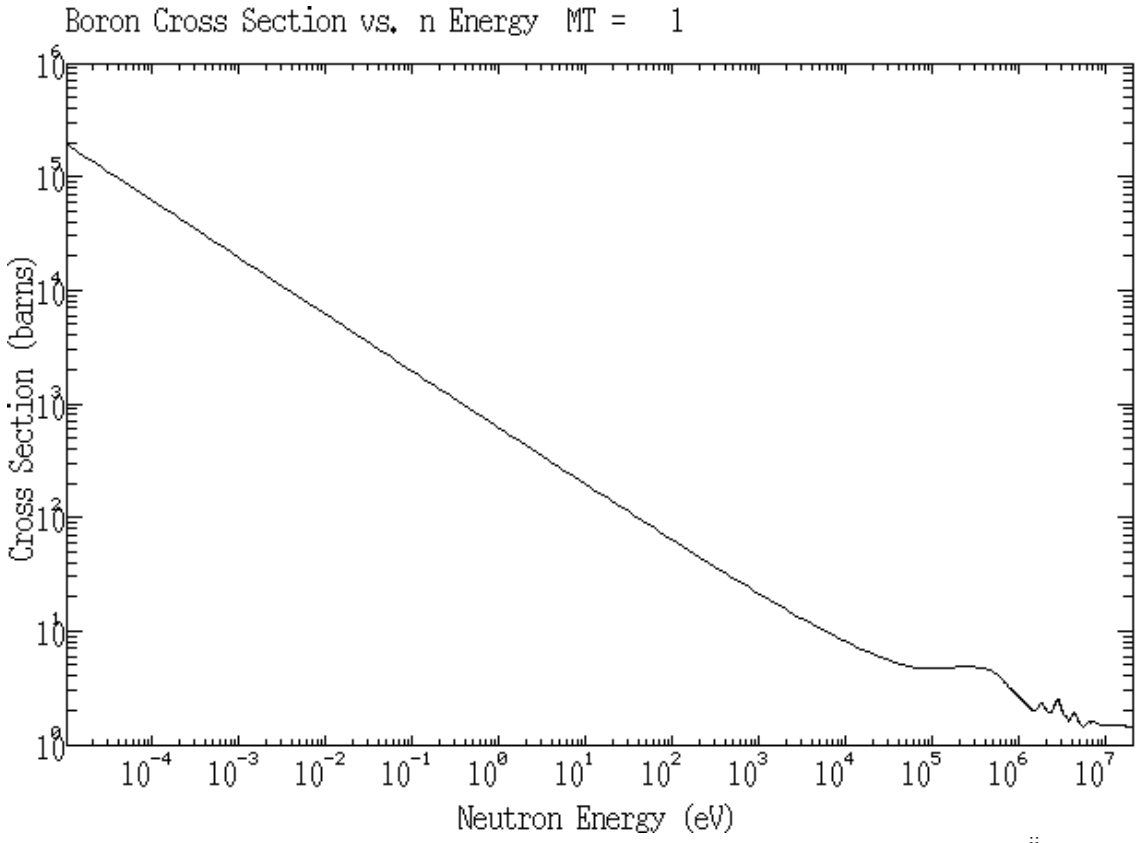

Figure 2-3 Sensitivity of Boron to neutrons vs. the neutrons' energy[ii]

the applied radial electric field. The negative charge is collected in the anode producing a current pulse (for an He^3 detector the neutron induced pulse is about 25 femto-coulombs). In a detector that is much larger than the stopping length of a proton in the fill gas, virtually all of the observed pulses would be the same height. Because detectors are usually limited to a size smaller than the stopping length of the charged recoil particles, not all of the kinetic energy of the daughter particles is collected. In a certain percentage of the interactions, one or both daughter particles will strike the wall before it deposits all its kinetic energy. The contribution of these events that deposit less than the full reaction energy on the anode can be seen in figure 2-2 as the "wall effect continuum." The smaller plateau is due to the triton and the larger one is due to the proton. More massive detection gasses such as BF_3 have less of a wall effect. Because the neutron absorption cross-section of Boron-10 (see figure 2-3) is weaker than that of He-3 in the thermal region, BF_3 detectors have lower neutron sensitivity compared to He-3 detectors. BF_3 detectors are also less sensitive than He-3 detectors to thermal neutrons because they must be operated at lower pressures. For the low intensity flux this project sought to measure, the increased sensitivity of Helium-3 was more useful than the decreased wall effect associated with boron trifloride. One method of decreasing the magnitude of the wall effect is to add a more massive gas, such as CO_2 to the primary fill gas. This increases the stopping power of the fill gas, increasing the chance that the particles will deposit their energy within the gas and not the wall. This added gas usually is less than ten per cent of the total fill gas and is known as the quenching gas.[i]

The other possible approach toward detecting neutrons involves scintillation detectors (see figure 2-4). A scintillator is a material that produces a small pulse of light when it is

Figure 2-4 BC-702 Thermal Neutron PMT Scintillation Detector by Canberra

stuck by a charged particle or a high-energy photon. Normally a neutron would pass inertly through a scintillator. To make the system sensitive to neutrons a scintillator such as a zinc sulfide phosphor is impregnated with a neutron sensitive element like Boron-10 or Lithium-6. The scintillator is fixed to a photo-multiplier tube (PMT) that senses the very faint bursts of light and amplifies them across increasingly biased plates known as dynodes. The pulses are then converted to an electrical signal that is fed into analyzer electronics. See appendix A for more discussion on PMT scintillator detectors. The key to every thermal neutron detection scheme is an element that has a high probability of an exothermic nuclear reaction when it absorbs a thermal neutron. The probability of a nuclear reaction is called its cross section. It can be thought of as the *effective* cross-sectional area of the nucleus. A thermal neutron detector will contain elements that are highly sensitive to thermal neutrons (that is they have a large cross section in the thermal region ~0.025eV) and less sensitive to higher energy neutrons. Figures 2-3 and 2-5 show the neutron cross-sections as a function of energy for two elements commonly used in thermal neutron detection.[ii] The noticeable characteristic of both elements is their large cross section in the thermal region that falls off strongly as energy increases. See appendix B, figure B-2, for the cross section of Lithium-6, which is also used in thermal neutrons detectors.

Thermal neutrons are those neutrons that have a velocity similar to the velocity of a gas molecule, a neutron energy of about 0.025 electron volts (eV). In order to detect only these low energy neutrons the detection system must have the ability to distinguish between low and higher energy neutrons. The difficulty arises in the fact that most neutron detection systems are sensitive, at least somewhat, to both fast and slow neutrons. As discussed above, the detection material can be chosen to maximize the cross section in the low energy region and minimize it in the higher energy region, however all available materials still will react to a number of particles above the thermal region. The accepted method of separating out the thermal flux from the total flux is to take two measurements. In one measurement the detection system is shielded from thermal neutrons by materials with a large, low-energy absorption cross-section (see discussion of shielding materials in chapter 3). The difference between the shielded and unshielded detectors is the thermal flux.

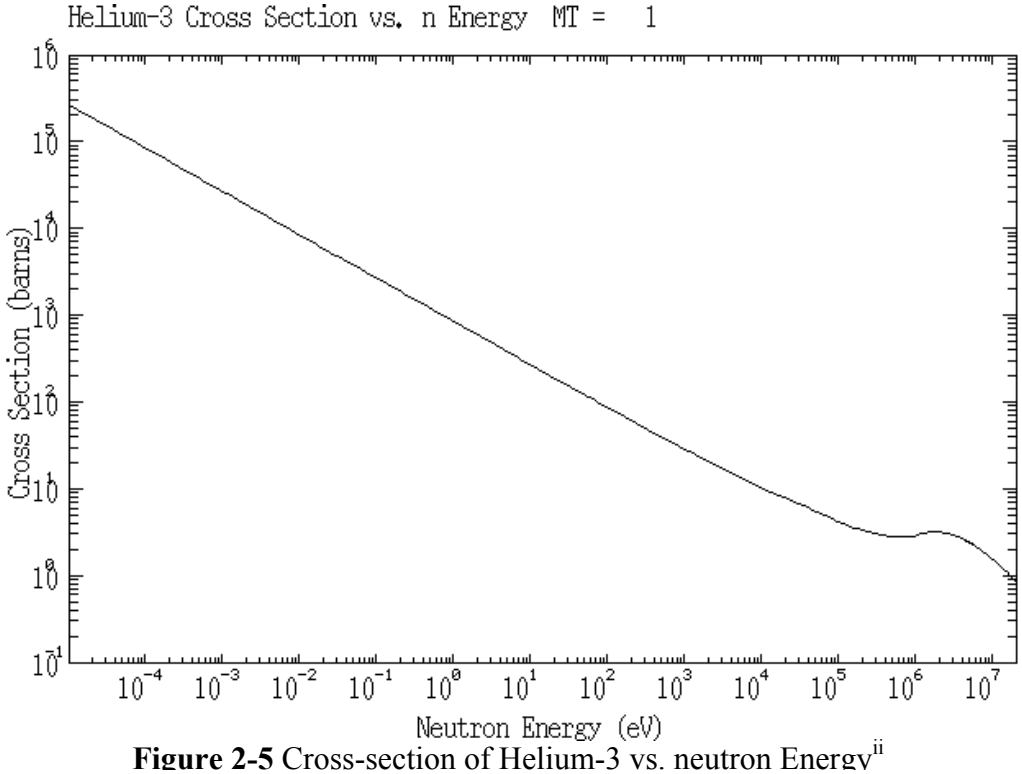

Figure 2-5 Cross-section of Helium-3 vs. neutron Energy[ii]

[i] G. Knoll, *Radiation Detection and Measurement*. 3rd Edition. New York: John Wiley & Sons, Inc.

[ii] Korean Atomic Energy Research Institute, Available online at http://hpngp01.kaeri.re.kr/CoN/endfplot.shtml, (APR 2002).

Chapter 3. The USNA Portable Thermal Neutron Detection System

This chapter discusses the Thermal Neutron Detection System (TNDS) designed and built for this Trident research Project.

System Development

Development of the USNA Thermal Neutron Detection System (TNDS) began with the scintillator PMT type detectors discussed in chapter 2, several of which were purchased. The scintillators used Lithium-6 as the neutron sensitive element. It was determined that these devices were unsuitable for the TNDS because of their sensitivity to gamma radiation, which made them difficult to calibrate. After the first calibration attempt the idea was abandoned in favor of ^{3}He gas-proportional tubes, which have very low gamma sensitivity.

Once the decision to use ^{3}He detectors was made, three different systems were independently developed. The first relied on traditional table-top laboratory equipment. The second design concept relied on miniaturized electronics, which were expensive and seem to have more of a problem with electronic noise. The third concept utilized two Ludlum digital programmable survey meters. After evaluation, the second design was eventually adopted; all are described below.

Figure 3-1 A typical NIMBIN

The USNA thermal neutron detection device is designed to be field-rugged, portable, and easy to use. In general, radiation detection equipment is composed of six major components: detector, pre-amplifier, amplifier, high-voltage power supply (variable), multi-channel analyzer, and

data collection processor or scalar counter. This equipment is modular and quite heavy when assembled. A rack that contains the main components of such a system can be seen in figure 3-1. In addition to the NIM-BIN (Nuclear Instrumentation Module Bin) seen in the figure, a preamplifier and computer with a multi-channel analyzer is required to make measurements. While such a setup is useful in a laboratory, its size and weight limits its usefulness when doing field measurements. A partial solution to this problem was found in the Inspector 2000 by Canberra. The Inspector is a portable piece of equipment that contains a high-voltage power supply (HVPS), an amplifier, and a multi-channel analyzer. It outputs its data in strings through a universal serial bus port (USB). The HVPS can provide up to a 1300 volt bias to a detector.

The USNA neutron detector package contains two Bicron ^{3}He gas-proportional detectors because two measurements are required to ensure that only thermal neutrons are being measured. One tube measured both the fast and thermal flux, and the other measured the fast flux only, because it was shielded from thermal neutrons. The thermal flux can be then calculated from the equation

$$\Phi_{thermal} = C \cdot \left(\dot{N}_{bare} - \dot{N}_{shielded} \right) \qquad \text{(Eq. 3-1)}$$

where $\Phi_{thermal}$ is the thermal neutron flux, $\dot{N}_{bare}$ and $\dot{N}_{shielded}$ are the count rate in the bare and shielded detectors, respectively, and C is a constant of calibration.

Being able to shield equipment from thermal neutrons is essential to properly measuring the thermal flux, and early in the project's development a determination of an appropriate shielding material was to be made. Shielding from low energy neutrons is best

accomplished through absorption by an isotope with a large thermal neutron cross-section. When a thermal neutron reacts with boron-10, for example, the following reaction occurs.

$$_5B^{10} + _0n^1 \rightarrow _3Li^7 + _2He^4 \qquad \text{(Eq 3-2)}$$

The product particles have a very short range through a solid. They deposit their energy through columbic interaction within the absorber and contribute very little radiation to the shielded area. Shielding from high-speed neutrons is more difficult, because they have smaller cross-sections (see appendix B). Thus it is necessary to slow the neutrons down (moderate them) in order to measure them. This moderation is best accomplished by materials with a large density and low atomic mass number atoms, because the scattering of the high speed neutrons is most energy depletive when the target atoms are on the same order of magnitude in mass as the neutron. Thus water or polyethylene makes a good moderator because of the high percentage of hydrogen ($m_H \approx m_n$). Thus imbedding a moderator with an absorber, or surrounding an absorber with a moderator, can slow fast neutrons with the moderator and then absorb them in the absorber, drastically lowering the total neutron flux.

An excellent choice for shielding thermal neutrons is cadmium. Natural cadmium is about 13% Cd-113. Cadmium-113 has a large thermal cross section (see figure B-1 in appendix B). Because Cd atoms are very massive when compared to a neutron, they are inefficient at moderating fast neutrons. This is extremely advantageous because the isotopes used in the gas-filled detectors are much more sensitive in the thermal region, and if the shielding material has a moderating effect then the fast neutrons would be over counted in the shielded detector leading to a falsely low thermal neutron count. The major disadvantage to

cadmium is its toxicity. Because the TNDS was intended to be portable and to operate in a non-laboratory, often populated, environment, an alternative to toxic cadmium was sought.

This project found an excellent alternative to cadmium in boron. Boron-10 also has a large thermal cross section (see cross section in figure 2-4). Because it is non-toxic, it is preferable for a mobile detection system. Boron impregnated moderators are common and are commercially available from nuclear materials vendors, where they are used to shield personnel and equipment from neutrons in radiation environments. Thus one of the two TNDS detectors is wrapped in 3/8 inch of Borated Silicate rubber manufactured by ThermoReax (see figure B-1 in appendix B). The Boron absorbs virtually all the thermal neutrons and through subtraction from the unshielded detector the thermal flux can deduced (equation 3-1).

The detector tubes are connected to two Ortec preamplifiers. The output of the detector consists of a **charge pulse** of about 30 μs in width. Because of the high voltage of the detector anode, considerable noise is also present. To extract the detector signal from the noise it is necessary to construct an electronic system to analyze the continuous stream of signals. This is done using standard commercial instrumentation that is modular and can be setup to process a wide variety of signals. The general outline of the standards of these modules is included in "Standard NIM Instrumentation System", U. S. Department of Commerce.[i] This document and a similar one by EGG/ORTEC were used as source material for the following discussion of electronic signal analysis.[ii]

The analysis of the signal is broken into two parts. The incoming signal is an analog electronic signal of a pulse of charge generated by the detector. First this signal is converted

to a voltage pulse. Then, the signal is processed with signal filters to exclude both low frequency noise and high frequency noise, isolating the narrow frequency band that contains the current pulse generated by the He-3 detector. Signals that make it through these band-pass analog filters are then converted to a special type of logic signals. These are rectangular voltage pulses of precise length, but whose amplitude varies with the voltage of the peak of the incoming analog signal. These pulses are precisely analyzed in amplitude and protocols are introduced to isolate only those signals within the band possible from the detector.

The preamplifier separates the high-voltage bias from the signal pulses and initially amplify and filter the signal. As discussed previously in the section describing the He-3 detectors, when a thermal neutron is detected a total of 764 keV of energy is released into electron-hole pairs. The conversion factor of this energy into charge is called the Fano Factor of a detector. For He this is somewhat large, about 5 eV/pair, which is significantly bigger than the 3.6 eV/pair found for silicon detectors. This means that the 764 keV released is converted to 153,000 electron-hole pairs. The detector is operated at a low bias, just enough to collect all the charge generated, but below the level where there would be any amplification by electron collisions. The 153,000 charges is the same as 25 fC, an extremely low charge pulse. The signal, along with extensive noise, is fed into a ultra-sensitive pre-amplifier which contains the first frequency filtration and then amplification. The pre-amplifier that is used is set to accept charge pulses from 1 – 40 μs in width. It amplifies these pulses approximately 40,000x, producing a sharp voltage pulse of about 250 mV in height. Since the pre-amplifier is an analog instrument, both the charge and the width of the He-3 pulse are retained in the output signal, however since this output is a voltage signal whose amplitude is proportional to

the incident charge, the correlation in both voltage and signal length is not one-to-one (see the upper plot shown in figure 3-2 below).[ii]

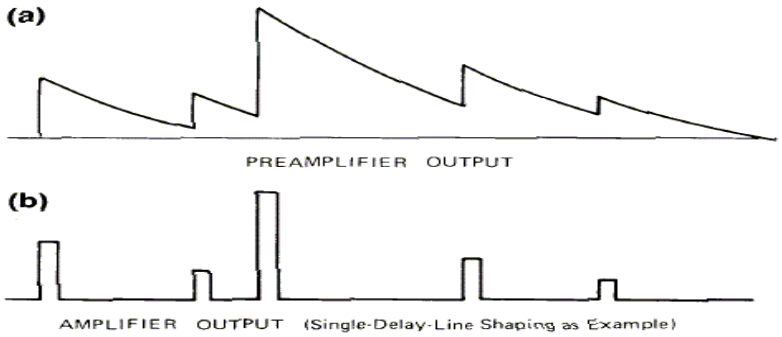

Figure 3-2 Output Pulse Shapes from (a) a Resistive-Feedback Preamplifier, and (b) the Delay-Line Shaping Amplifier Connected to the Preamplifier.

This figure illustrates the typical output pulse shapes from a resistive-feedback pre-amplifier. The output for each pulse consists of a rapidly rising step, followed by a slow exponential decay. It is the amplitude of the step that represents the energy of the detected radiation. Although normally the decay time of nuclear detection signals is relatively short, less than 30 μs, the USNA TNDS used a considerably longer decay time (38 μs) because the count rate was so low and the system could afford to use long times for a more precise signal analysis.

The signal is then fed into an amplifier that will perform more extensive signal processing to eliminate noise pulses, and then to add an additional amplification of 10x to 30x so that the final output signal has a voltage amplitude of about 5 volts.

The problem is that even though the expected count rates are a few per second, noise of the size of the detector signal occurs continuously, and the pulses pile up on the tails of previous signals. The amplifier filtration is based on standard RC time constants to create a frequency window as shown in Figures 3-3 and 3-4 below.

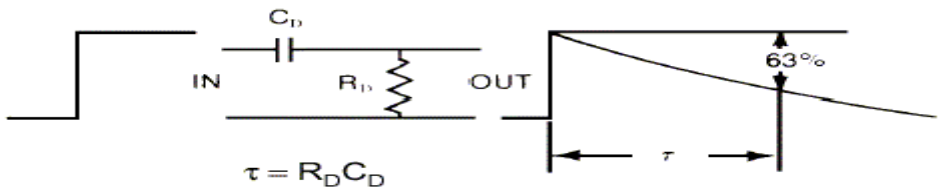

Figure 3-3 CR Differentiation

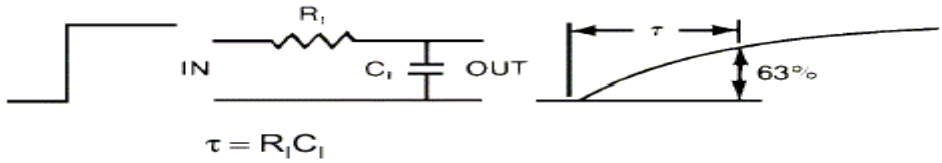

Figure 3-4 RC Integration

First the signal from the pre-amplifier is passed through a CR, high-pass filter as shown above. Figures 3-3 and 3-4 are simplified to enable the discussion below. The actual circuit is far more complex. This improves the signal-to-noise ratio by attenuating the low frequencies that contain mostly environmental noise. This kind of noise generally is found on electrical supply lines, for example the common 115V AC lines, and come from distant sources such as lightning, power tools, arc lighting, etc. This kind of circuit filtering is called a "differentiating filter" because it acts similar to the mathematical equivalent of differentiation. When a complex signal is differentiated, the slow signals approach constant DC values, and can be eliminated by transmission through a capacitor. The "time-constant" of the differentiation can be adjusted, and by setting a value of about 1 μs, all noise below about 1 MHz can be sharply attenuated. In practice, a time-constant of 38 μs was found to give optimal reduction of low-frequency noise while retaining the signal integrity of the He-3 detector signal.

After the CR filter shown in figure 3-3, the signal is fed into an RC type filter circuit shown in figure 3-4. This filter acts as a low-pass filter that attenuates all the high frequency

noise. Such noise is very prevalent, especially from RF signals from TV and radio stations, as well as cellular telephones (0.9-1.6 GHz). This filter acts similarly to the mathematical equivalent of integration. Integration averages over a time interval. If a time constant of 1 μs is selected, then the filter will attenuate signals above 1 MHz. For integration, the He-3 detector system showed optimal response to a low-pass time constant of 10-30 μs.

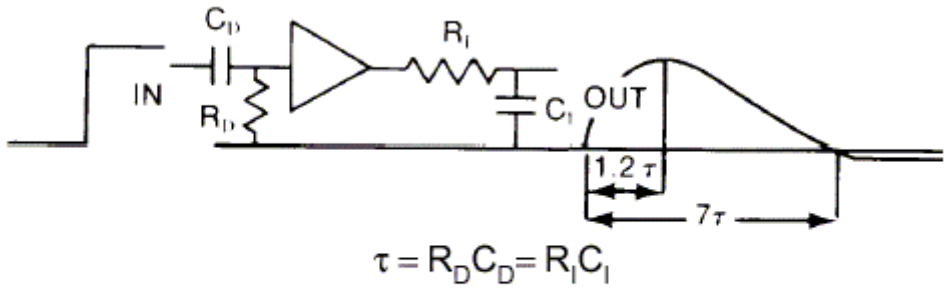

Figure 3-5 CR-RC Pulse Shaping

Figure 3-5, above, shows the effect of combining the high-pass and low-pass filters in an amplifier to produce a unipolar output pulse. Typically, the differentiation time constant, $\tau_1 = R_D C_D$, is set identical to the integration time constant, , $\tau_2 = R_I C_I$. The output pulse rises slowly and reaches its maximum amplitude at about 20% longer time than the time constants. The decay back to the baseline is controlled primarily by the time constant of the differentiator. This simplified circuit analysis does not compensate for the long time constant of the pre-amplifier decay time. If this circuit was used as described above, there would be significant undershoot of the output signal because of this decay time. However, compensating circuits are also included which reduce this overshoot to tractable levels.

The final step in the electronic analysis of the He-3 detector output signals is to send the filtered and amplified signals into a multi-channel analyzer. This instrument has an input

module which functions as an analog to digital converter. It operated by having a lower-level threshold (signals less than this amplitude are ignored) which gates out low level noise. It then precisely measures the peak signal heights and digitizes these. The memory of the multi-channel analyzer consists of up to 2^{15} separate counters. The digitized signal is scaled to correlate with one of these counters, and that counter is incremented. For example, if the total accepted signal amplitude is 10 volts and the signal output of the amplifier is 5 volts and the multi-channel analyzer is set at 1024 channels, then the counter corresponding the channel 512 will be increments by one to indicate a pulse was received whose pulse height fell into the narrow range of 4.904 – 5.096V (each counter correlates to a voltage width of 10V / 1024 counters).

The final result is shown in figure 3-6 below.

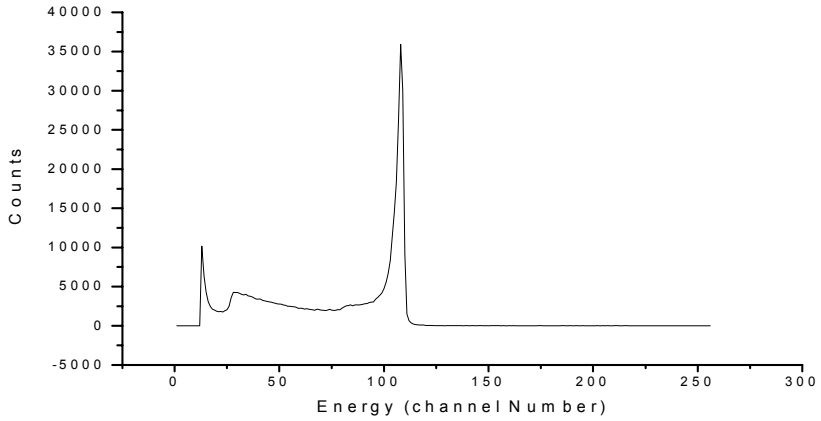

Figure 3-6 Data collected from a Helium-3 Tube Displayed as Histogram

This plot is a typical multi-channel analyzer distribution for the He-3 detector under optimal signal processing. The peak contains the signals from the $He^3 + n \rightarrow H^3 + p$ nuclear reaction described previously. If all the electrons from the electron-hole pairs are collected by the central anode of the detector, they will be processed to be recorded in channel 105 as

shown. The slight channel width is due to underlying noise that slightly changes the final signal voltage.

To the left of the sharp major peak is a long ledge trailing down to low energies, ending at channel 25. This ledge contains pulses from events in which one or both of the particles from the nuclear reaction impinge the detector wall before it loses its energy. The mean free path of the 573 keV proton in He-3 gas at 4 atmospheres, which is the pressure in the He-3 detector used in this project, is about 2 cm. This is the radius of the detector. Hence, about half of these particles will impinge into the wall before it loses all its energy. Since the wall is metallic at ground potential, any residual electron-hole pairs produced here are lost. Therefore, about half of the total counts of the reaction reside in the ledge below the peak, and this represents incomplete collection of charge.

Below this ledge the counts drops to about zero, showing just a few counts from noise that gets through all the filtration. At the lowest energies, below channel 20, the counts begin to increase from the natural electronic noise at very low voltages. The system has a cut-off at about channel 10, described above as a low-level discriminator. This eliminates most signals from the electronic noise.[ii]

The Canberra Inspector 2000 provides high-voltage to the detectors and low-voltage to the pre-amps as well as receiving the signal from the pre-amp, amplifying it (converting it to square pulses of varying heights) and then binning the pulses by their magnitude. The extensive gain, integration/differentiation control discussed above all takes place within the Inspector and are controlled by the software discussed below.

The two Inspectors feed their data streams via independent USB to a Micron PC laptop. A complete layout of the USNA TNDS electronics appears in figure 3-7. The computer uses Genie-2000, a program produced by Canberra to record the pulses and their energy. It then produces a histogram from the data in near real time. The computer can receive data streams from each independent detector setup simultaneously. Figure 3-8 depicts the USNA TNDS open and ready for measurement. The photograph, however, only displays the most accessible elements.

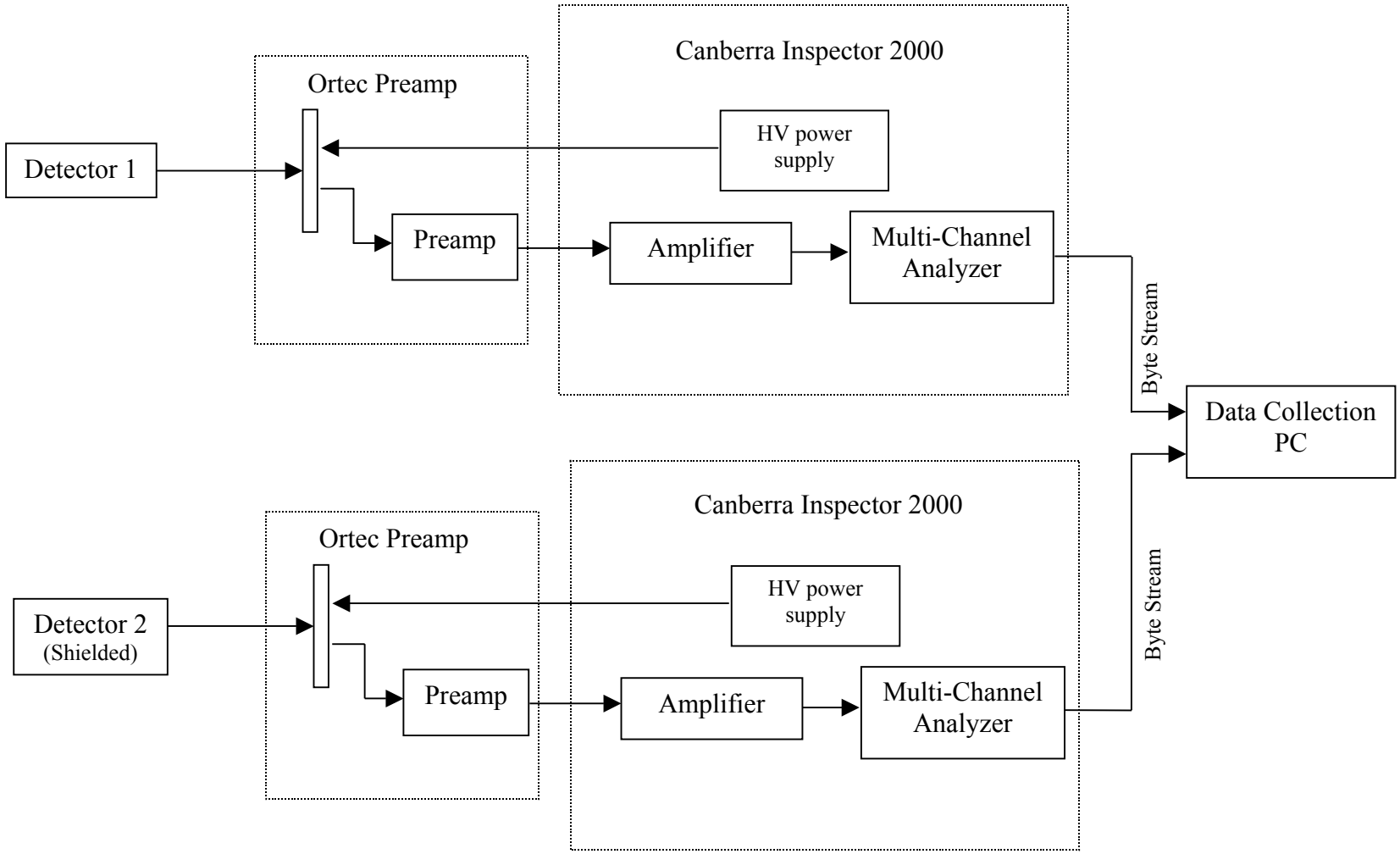

Figure 3-7 Block Diagram of the USNA Thermal Neutron Detection System.

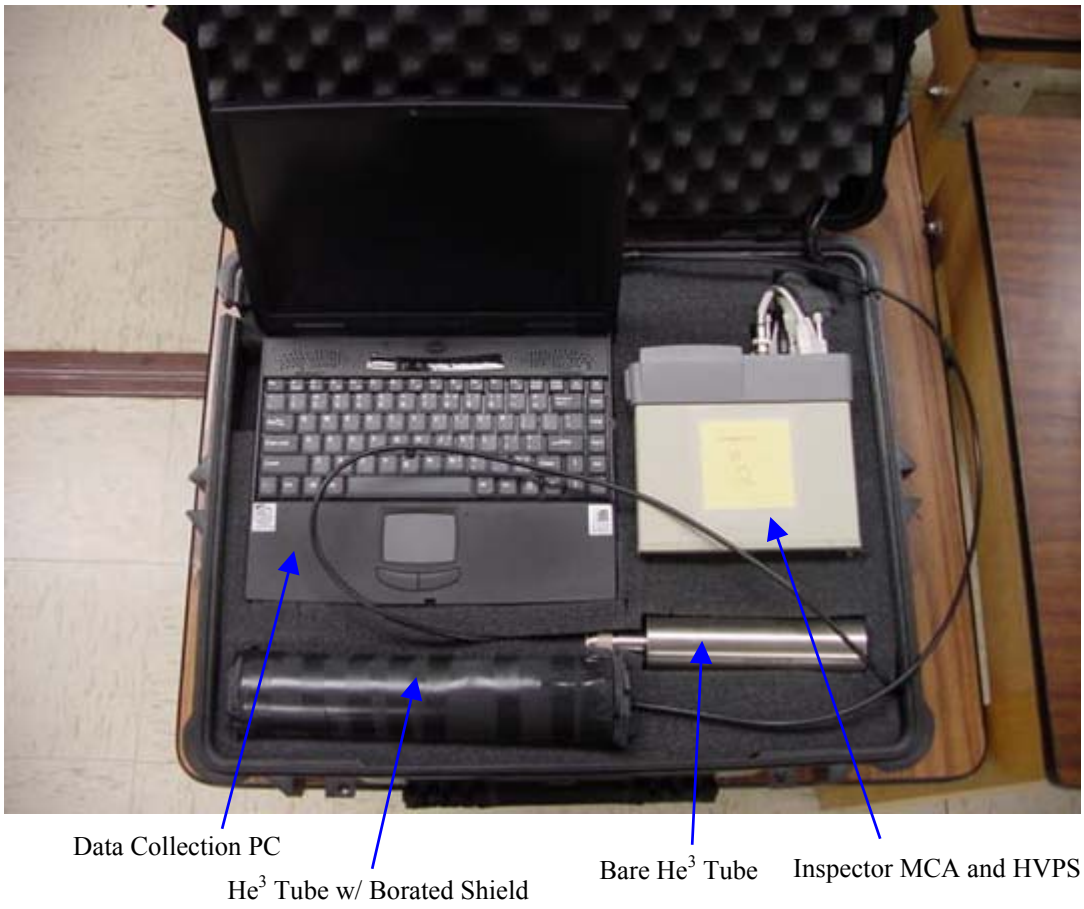

Figure 3-8 The USNA Thermal Neutron Detector System ready for transport or measurement

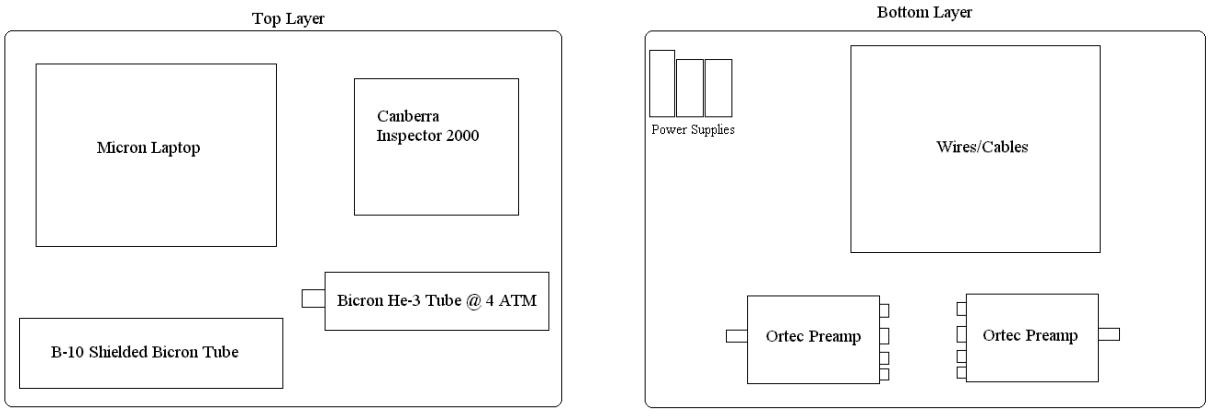

Figure 3-9 The layers of the Thermal Neutron Detection System

Beneath the upper layer shown are pre-amps, power supplies, and several meters of cable. The layout of the layers can be seen in figure 3-9.

A typical spectrum produced by the Canberra system is displayed in figure 3-12. The data can be either integrated to attain a scalar count, or the data can be extracted in tabular format for analysis.

The scalar number derived from the spectra of the USNA TNDS is determined by selecting a part of the spectrum that is easily identifiable as pulses registered from neutrons interacting with the detector, but that is not too cluttered by noise. The majority of the counts are in the primary reaction peak shown in figure 3-10. This peak represents the reactions that deposit most of their energy in the detector gas (see chapter 2). A significant fraction of the counts lie in the wall effect region, however. For consistency, the number used for calibration and field measurement was the integral number of counts from the highest energy channel of the peak to the channel whose value is one half as great. This area is called the region of interest (ROI). For example, in figure 3-10 the highest channel of the peak was measured at 110, then the number of counts registered during the data run would be the integral number of counts from channel 55 to channel 110.

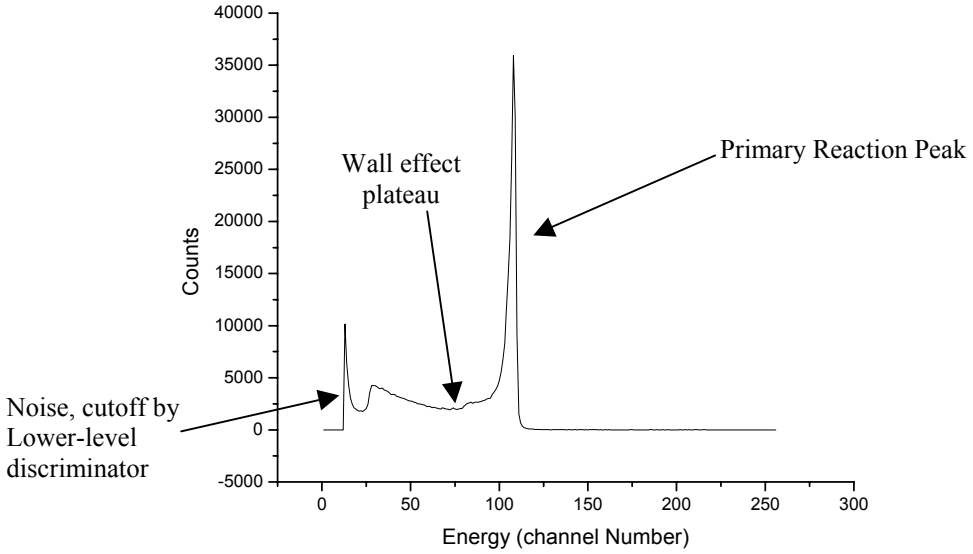

Figure 3-10 Typical reaction product spectrum from He^3 based USNA Thermal neutron detection system Note the wall effect plateau (discussed in "Detectors" section) and the noise peak

Another approach in the search for a portable thermal neutron detection system was to use commercial survey meters. Two Ludlum 2350 digital programmable survey meters were purchased and outfitted with Bicron ^{3}He tubes identical to those used in the Canberra and NIMBIN systems. Because of their small size and extremely small weight, the survey meters promised excellent portability and practicality. The survey meters operated on four 'D' type batteries and provided their own high voltage bias to the detector tubes. All amplification and signal discrimination took place within the handheld unit. The units had a threshold (low level discriminator) and a window (maximum energy counted) adjustments, but provided only a scalar count (opposed to spectral data) of events detected by the electronics. The Ludlums could be programmed to take data points over time that could be downloaded by computer at a later date. While evaluating this system an upward trend in the count-rate of the detectors in the constant neutron field of the USNA sub-critical reactor was observed (see figure 3-11).

Under the assumption that this was an effect of the draining batteries, the manufacturer was requested to outfit the detectors with wall power adapters, which they did at a small cost. With continued experimentation it was determined that only a bias voltage well above the optimum range for the tube would yield significant efficiency (count rate for a given flux). To remedy the problem the gain of the detector was physically increased to its maximum. However, this setting lead to self-induced electronic noise problems. After many weeks of effort the Ludlum system was abandoned.

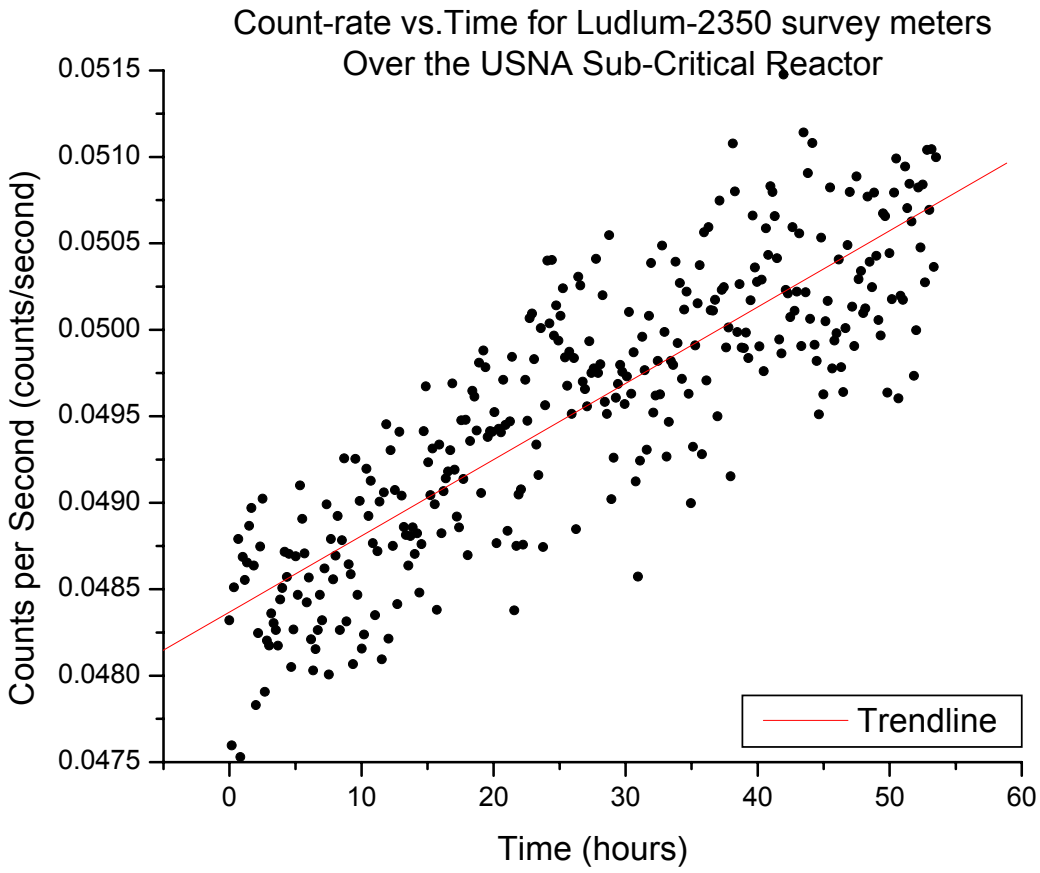

Figure 3-11 The Count-rate over time for Ludlum-2350 survey meters with Bicron He-3 tube. An effort was made to use Ludlum model 2350 Survey meters to measure the ambient thermal neutron flux. One problem encountered was a variation in the detector count rate with time. This figure illustrates the problem. The survey meter approach was developed simultaneously with the eventual detection system. This approach was abandoned after problems with self-induced noise at high gain and low count rates could not be resolved. The neutron field was constant over time and produced by the Naval Academy's sub-critical natural uranium reactor.

Measurement Protocol

Constructing, evaluating, and calibrating the detection system occupied the majority of the project's energy for its first three months. The Canberra detection system initially detected two peaks, instead of the single 764 keV reaction peak from the n + He^3 reaction. The project considered staying with the NIMBIN based setup, which was functional, although the equipment weighed several times more. Through experiment, however, the Inspector system was eventually properly configured to eliminate the second, false peak.

After assembling a working system electronically, it was necessary to build and package the physical system. To ensure that the case and foam that the system uses for packing would not moderate fast neutrons, or contribute a significant shielding effect, an experiment was performed. First, two detectors were placed in the sub-critical reactor room at USNA. The reactor provides a constant low intensity poly-energetic neutron flux. A control run was first performed by taking a measurement with two detectors operating half a meter apart and ten meters from the reactor. In a second run, one of the detectors was placed inside the case, and the other was left uncovered. By comparing the ratios of the detectors with and without the case any shielding effect would be seen. The result of this experiment was that the fluxes differed by less than half of one percent, which is within the statistical counting error. The conclusion that the case had a negligible effect was borne out at NIST where comparison experiments showed virtually no variation in counts when the lid was either open or closed (see figures 3-12 and 3-13).

During the course of shielding evaluations it was determined that the pre-amplifiers varied in gain by as much as 15%. Analysis was performed to place the principle reaction

peaks within a few channels of each other by adjusting the fine gain of the amplifier that was to be used with a specific pre-amp.

Calibration experiments were performed at the Naval Surface Warfare Facility in Carderock, MD, at National Institute for Standards and Technology (NIST) in Gaithersburg, MD, and at the Armed Forces Radiobiology Research Institute (AFRRI) in Bethesda MD. The most important of these experiments are described in chapter four “Calibration.”

-

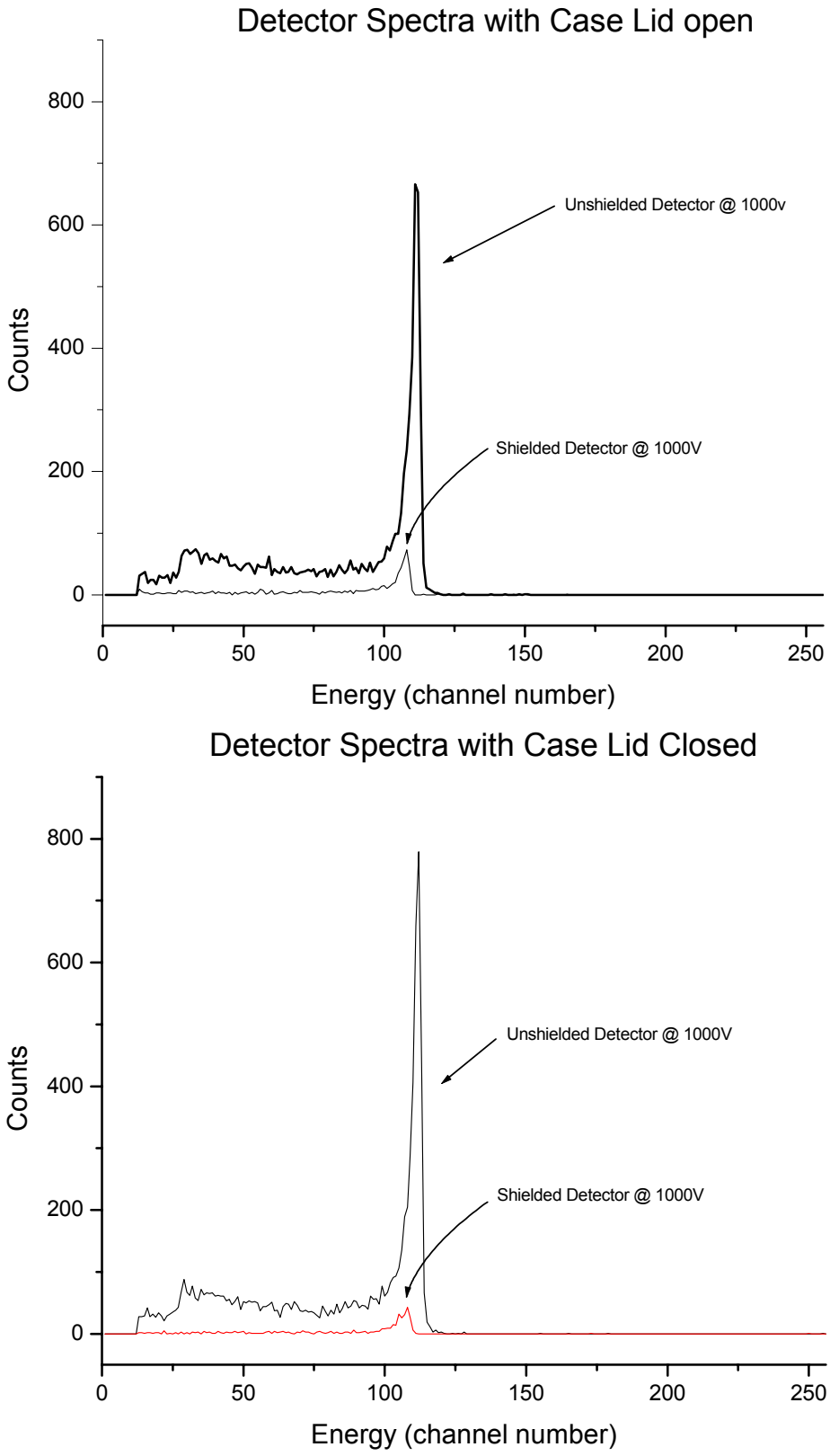

Figures 3-12(Top) and **3-13** showing the small variation caused by the TNDS' Case

The final field measurement protocol was established based on the time spent developing and evaluating the system.

FIELD MEASUREMENT PROTOCOL FOR USNA THERMAL NEUTRON DETECTION SYSTEM

Power Supply: 120VAC

MCA/HVPS: Canberra Inspector 2000

Preamp: EG&G ORTEC 142PC Preamp

Detector: SAINT-GOBAIN (BICRON) 4 ATM HE^3 model number 15He3-304-50HN

Data Collection: Simultaneous Two Tubes w/ Genie Data Collection Software by Canberra

System Setup: Tubes in Case, Case Lid Open

Time Constant (τ_c): 38μs

Tube Bias: 1000 VDC

Tube Connection: 50-ohm coaxial cable with C-type to SHV (3 foot) connectors

Course Gain: 5x

Fine Gain: Inspector 1 0.9996

Inspector 2 1.1488 (To correct for differences in preamp gain)

Super-Fine Gain: 0.999998

[i] DOE/ER-0457T, U. S. NIM Committee, May 1990. Report available as "Standard NIM Instrumentation System," NTIS, U. S. Department of Commerce, Springfiled, VA, 22161.

[ii] All electronic schematics from the section entitled "Signal Processing Electronics" are taken from the EGG-Ortec Electronics Catalog, 2001, or from their website: www.ortec-online.com.

Chapter 4. Calibration

The thermal flux measured by the USNA Thermal Neutron Detection system is calculated according to equation 4-1.

$$\Phi_{thermal} = C \cdot \left(\dot{N}_{bare} - \dot{N}_{shielded} \right) \qquad \text{(Eq. 4-1)}$$

Where $\Phi_{thermal}$ is the thermal flux in units of neutrons / cm^2-s, $\dot{N}_{bare}$ and $\dot{N}_{shielded}$ are the count rates measured in the region of interest for each tube, and C is the calibration constant. The calibration constant relates the count rate of the detector to the value of the neutron flux measured. The calibration constant depends on the efficiency of the detector, that is the fraction of neutrons that enter the detector and cause a measurable event. The calibration constant has units of neutrons per square centimeter per count. In order to determine a calibration constant for a particular detector, the detector must be operated in a known flux environment. Then from the count rates of the bare and shielded detectors and the known flux, the calibration constant can be calculated as in equation 4-2.

$$C = \frac{\Phi_{thermal}}{\dot{N}_{bare} - \dot{N}_{shielded}} \qquad \text{(Eq. 4-2)}$$

where $\dot{N}_{bare}$ is the bare count rate and $\dot{N}_{shielded}$ is the count rate of the shielded detector.

Initially, the calibration was thought to be simple since thermal neutrons are widely used in a variety of research projects, as well as the myriad detectors available for use near nuclear reactors. As this project shows, the setups used at national laboratories were all only crudely calibrated and none agreed within a factor of 2x with each other. We have found that calibrating a thermal neutron detection device is very difficult, and it took many trips and the full length of this Trident project to obtain satisfactory results. Calibrating a thermal neutron

detection device is difficult because there exist few well-calibrated thermal neutron sources. The best-calibrated thermal neutron source is possibly the thermal column off the nuclear reactor at NIST. Unfortunately, this facility was down for maintenance during the duration of this project. This project visited three facilities to attempt calibration: the National Institute of Standards and Technology (NIST) (Formerly the National Bureau of Standards) in Gaithersburg, MD; the Naval Surface Warfare Center (NSWC), Carderock, MD; and the Armed Forces Radiobiology Research Institute (AFRRI) in Bethesda, Maryland AFRRI operates a 1 megawatt TRIGA (**T**raining, **R**esearch, **I**sotope, **G**eneral **A**tomic) reactor with a neutron beam. Discussion of the two most important calibrations, those at AFRRI and NIST, follows. The NSWC calibration is not discussed because it produced a calibration factor an order of magnitude greater than either of the other two facilities. A major difference in the irradiation set-up existed between NSWC, Carderock and both NIST and AFRRI. At NSWC, Carderock the neutrons were produced by colliding high-energy protons into a beryllium target, which then produced fast neutrons. These fast neutrons where then moderated in heavy water. The result of this process was to create a thermal neutron beam that was nearly monodirectional in orientation on the USNA thermal neutron detector. In contrast, at both AFRRI and NIST the thermal neutrons were produced predominately from room return off concrete walls. Hence in these two later situations, the thermal neutrons seen by the detection equipment were diffuse, which is a situation much closer to what would be found in a real world environment. For this reason, a large difference in the calibration coefficient was obtained at NSWC, Carderock then at the other two facilities. Hence, the NSWC, Carderock calibration coefficient is considered to be much less credible and not used further in the project.

NIST Low Scatter Room Calibration

In order to obtain a calibration factor for the detectors' response to thermal neutrons experiments were conducted at the National Institute of Standards and Technology (NIST) (formerly the National Bureau of Standards) in Gaithersburg, MD. The scientists at NIST are the recognized experts in measurement technology. The facility has a Low Scatter Room equipped with several Californium sources of varying strengths. The room is ten by ten by three meters. It is below ground with concrete walls. In a high flux environment, such as that of a nuclear reactor (see "AFRRI Calibration"), the detector can become saturated because of its high sensitivity, which is not desirable for calibrating the system. Californium-252 is a self-fissioning fast neutron source, which can be moderated to produce thermal neutrons. NIST has several Californium sources with strengths as high as 200 mrem/h at one meter. The Cf sources are stored below the floor for the safety of personnel working in the room. The source was raised by a string into a sphere of heavy water (D_2O) (see Appendix B for the cross-section of deuterium). The heavy water provides some initial moderation of the neutron flux without absorbing nearly any neutrons (see discussion of slowing fast neutrons in Chapter 3). Most of the neutrons are finally slowed to thermal energy when they collide with the walls and are moderated by interactions in the concrete. This phenomenon is known as "room return." Because the thermal neutrons are produced mostly from the walls, the low scatter room at NIST is a near-uniform thermal neutron environment. This is an ideal since natural background neutrons are largely uniform.

Calibration experiments with the USNA TNDS in the NIST ^{252}Cf room were performed on 6 November 2001. Graphs of experimental data appear in Figures 4-1 through

4-4. The neutron detector was placed on a steel platform at the same height as the heavy water sphere (see Figure 4-5). The data collection PC was positioned so it was visible by closed circuit television in the control room. Data collection was started manually in the ^{252}Cf room. To initiate the experiment a fishing reel drew up the californium source into the heavy water sphere. The integral number of counts in the region of interest collected prior to the source seating in the D_2O sphere was noted. These counts were produced in the approximately three seconds required for the source to rise, unshielded, the 3 meters from the source storage block to the moderator sphere. Several measurements were then taken at different tube biases and with different time constants as shown in table 4-1. By taking the percent difference between the fourth run and the tenth (data given in table 4-1), it can be seen that the measured flux varies only 13% with rotation, which is within the expected spatial variation of the flux in the ^{252}Cf room.

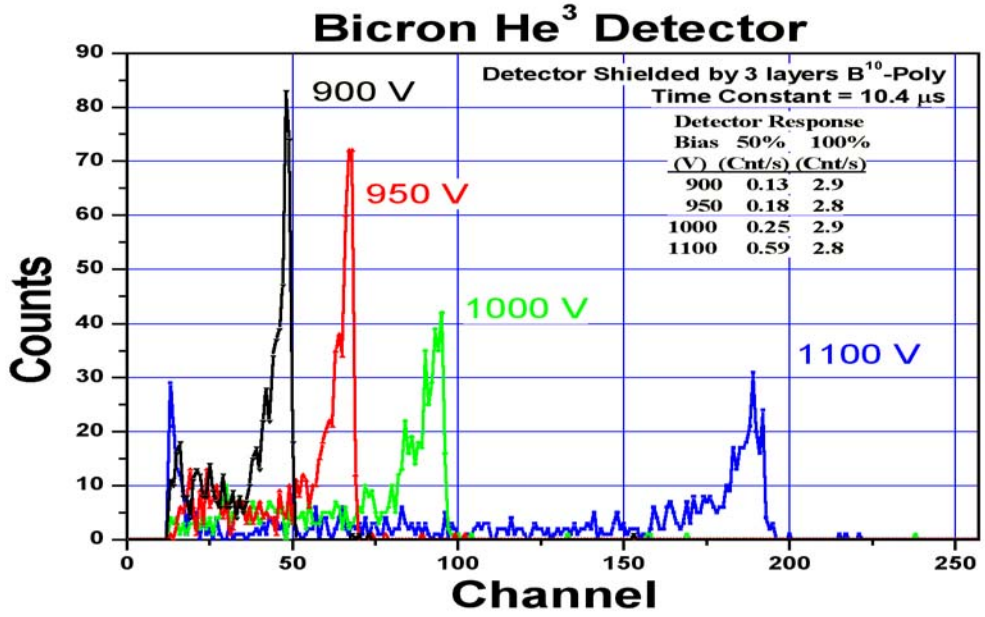

Figure 4-1

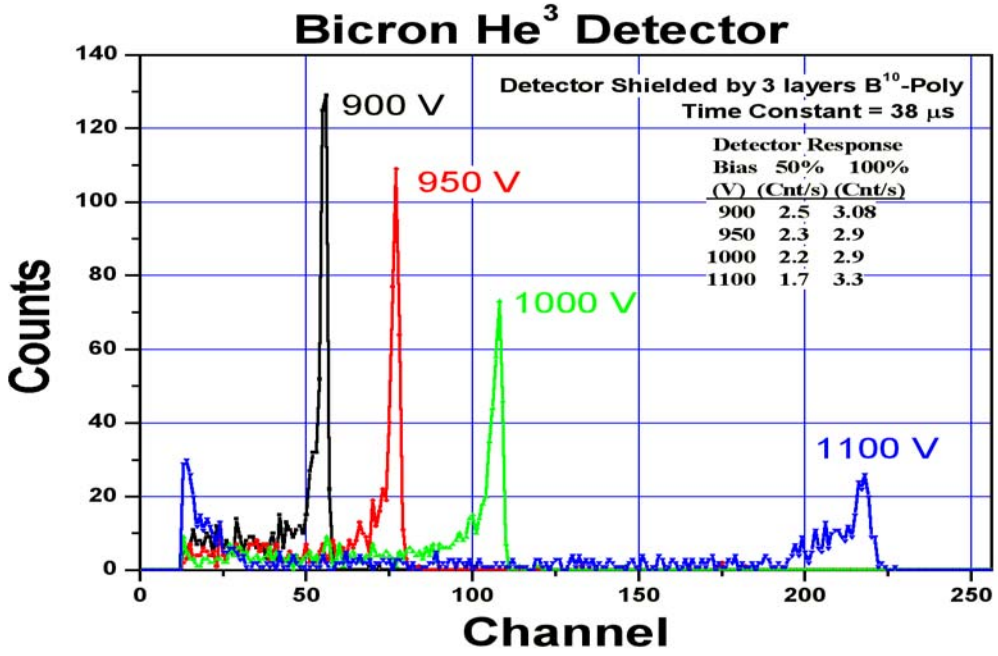

Figure 4-2

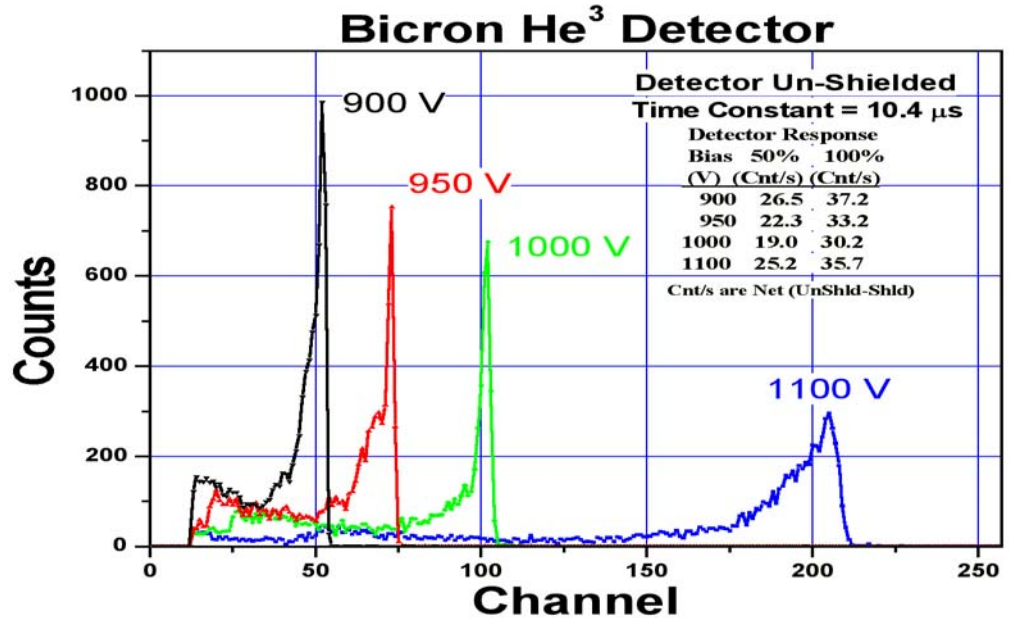

Figure 4-3

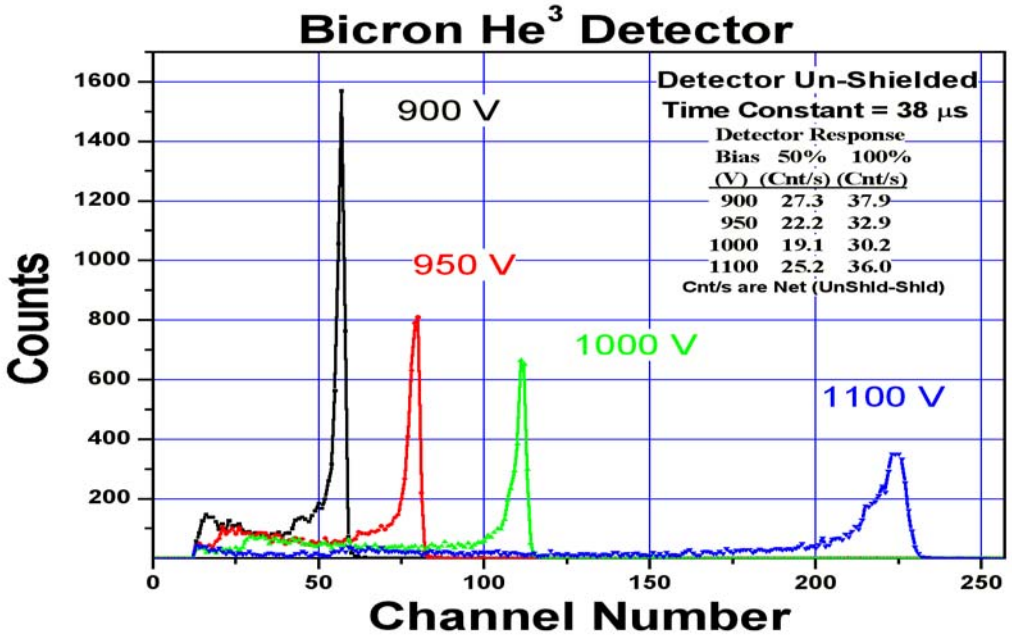

Figure 4-4

Data Collected at NIST Calibration

run	Tube Bias	T_c	Bare	1σ Uncertainty	Counts in 4 min w/ Borated Shield	Net Thermal Counts	Comments
1	1000V	38μs	5071	±1.4%	552	4519	
2	900V	38μs	7000	±1.2%	596	6404	
3	950V	38μs	5686	±1.3%	525	5161	
4	1000V	38μs	5065	±1.4%	549	4516	
5	1100V	38μs	6378	±1.3%	409	5969	
6	1100V	10μs	6354	±1.3%	424	5930	
7	1000V	10μs	4984	±1.4%	514	4470	
8	950V	10μs	5828	±1.3%	555	5273	
9	900V	10μs	6771	±1.2%	528	6243	
10	1000V	38μs	5458	±1.4%	331	5127	Detectors Rotated 90 deg
11	1000V	38μs	6226*	±1.3%	657	5569	Case lid closed
12	1000V	38μs	5487	±1.3%	N/A	N/A	With shielded detector removed

*This value is somewhat less accurate as the closed lid prevented accurate zero-point correction

Table 4-1

The thermal neutron flux in the low scatter room at NIST was calibrated using a Livermore type ^{235}U fission chamber by Dr. Alan Thompson of NIST at the exact location where the USNA TNDS had been positioned. The fission chamber contains 0.18 grams of ^{235}U and is filled with P-10 gas. Uranium-235 has a strong neutron cross-section (see Appendix B). When a neutron strikes the detector a fission of a ^{235}U atom is likely to occur and the released energy (in the form of ionizing fission products) is collected by the P-10 gas (see discussion of gas-proportional counters, chapter 2). The produced charge pulse is collected and counted.

The calibration took place in two parts. First the fission chamber was operated in the room bare. Then it was operated wrapped in 0.025 inch thick cadmium foil, which corresponds to 7.3 stopping lengths for thermal neutrons. In this case less that one tenth of a percent of the neutrons with energy less than 0.3 eV penetrated the cadmium shield. Faster neutrons, however, were transmitted. By subtracting the shielded counts measurement from the unshielded counts, the net thermal counts could be determined.

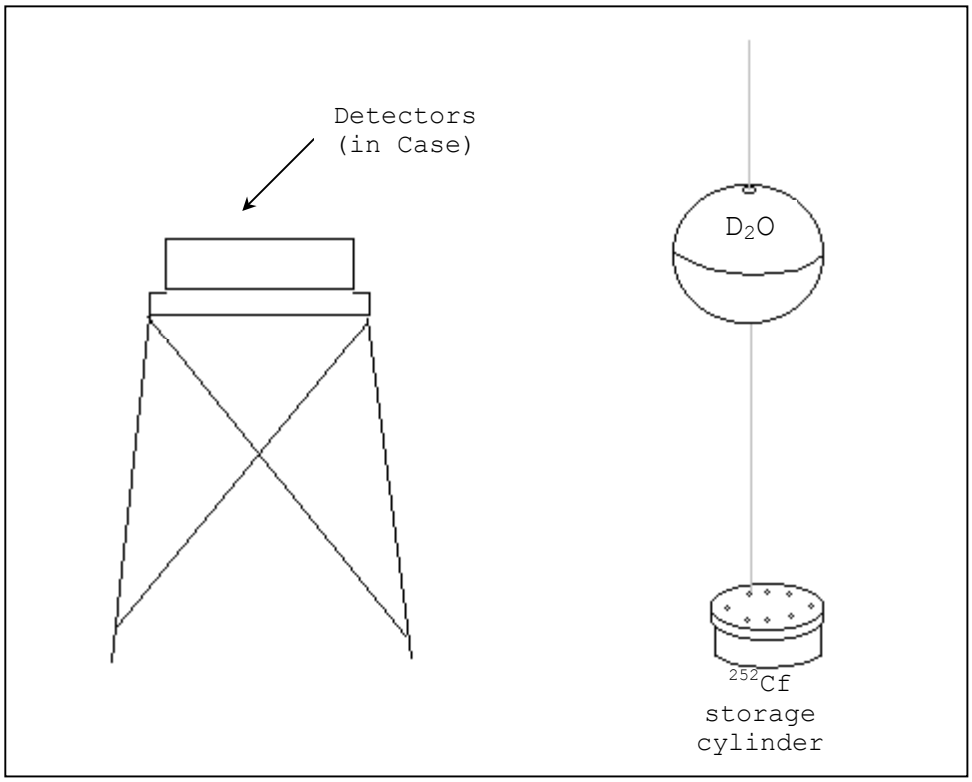

Figure 4-5 The Low Scatter Room at the National Institute of Standards and Technology is equipped with multiple Californium-252 sources that can be drawn up into a heavy water moderator sphere. The concrete that make up the walls of the vault moderated the fast neutrons from the Californium-252 and created a thermal flux in the room. The thermal component of the flux was measured using a Urainium-235 fission chamber. The USNA Thermal Neutron Detection System in its measurement/travel case was placed on a high steel stand in the center of the concrete vault. A calibration constant for the detection system was obtained.

Dividing the mass of ^{235}U in the fission chamber by its gram-molecular mass and multiplying by Avagadro's number (*N*) revealed that there were 4.6 x 10^{20} uranium atoms are present in the detector, as shown below:

$$\frac{0.18g}{235\,{}^{g}\!/_{mol}} \cdot N = 4.6\times10^{20}\,atoms \quad \text{(Eq 4-3)}$$

The effective target area of the uranium in the detector (A_{eff})is the product of the number of atoms and its average microscopic cross-section σ_{f235} (see equation 4-4).

$$A_{eff} = N_{atoms} \cdot \sigma_{f235} \qquad \text{(Eq 4-4)}$$

The NIST low scatter calibration initially assumed a microscopic fission cross-section of 500 barns. According to equation 4-4, the effective target area of the detector is 0.226 cm^2.

The source used in the Low Scatter room calibration had a strength of 1.99 x 10^8 neutrons per second. The fission chamber was irradiated for 50 seconds for each data collection run. The detector registered an average of 820 counts in the fission chamber per bare run, and 220 counts per shielded run. According to equation 4-5 the thermal count rate is then 12 counts per second.

$$\dot{N}_{thermal} = \dot{N}_{bare} - \dot{N}_{shielded} = 12\,{}^{counts}\!/_{s} \qquad \text{(Eq 4-5)}$$

The thermal flux for the room calibration, $\Phi_{high\text{-}thermal}$, at the fission chamber is then determined according to equation 4-6 to be 53 neutrons per square centimeter per second.

$$\Phi_{high-thermal} = \frac{\dot{N}_{thermal}}{A_{eff}} = 53\,{}^{n}\!/_{cm^2\cdot s} \qquad \text{(Eq 4-6)}$$

Where $\Phi_{high\text{-}thermal}$ is the thermal flux in the low scatter room when the source of high neutron output is in use. The californium source used to calibrate the sensitive USNA TNDS only

emitted 2.1 x 10^6 neutrons per second. Thus to find the thermal flux at the calibration location for the TNDS run, $\Phi_{thermal,}$ the thermal flux measured by the fission chamber must be scaled by the ratio of the source strengths, *S*. The result of this process is given by equations 4-7 and 4-8 below.

$$S = \frac{1.99 \times 10^8 \, {}^{n}/_{s}}{2.1 \times 10^6 \, {}^{n}/_{s}} = 94.76 \qquad \text{(Eq 4-7)}$$

$$\Phi_{thermal} = \frac{53 \, {}^{n}/_{cm^2 \cdot s}}{S} = 0.56 \, {}^{n}/_{cm^2 \cdot s} \qquad \text{(Eq 4-8)}$$

At 1000 volts with a time constant of 38μs (the standard chosen for measurement during equipment evaluation) the TNDS measured 30.2 counts per second (cps) in the bare tube and 2.9 counts per second in the boron shielded tube. Referring back to equation 4-2 the calibration coefficient for the USNA TNDS can be calculated.

$$C = \frac{\Phi_{thermal}}{\dot{N}_{bare} - \dot{N}_{shielded}} = \frac{.56 \, {}^{n}/_{cm^2 \cdot s}}{30.2 \, {}^{cnts}/_{s} - 2.9 \, {}^{cnts}/_{s}} = .020 \, {}^{n}/_{cm^2 \cdot cnt} \quad \text{(Eq 4-9)}$$

The Calibration Constant Determined at the NIST low scatter Room

The uncertainties involved in the calibration highlight the difficulty in getting a good thermal neutron calibration. First the assumption that the microscopic cross-section for uranium-235 is 500 is uncertain to –40% and +200%. The ^{235}U fission cross-section for neutrons at 0.025 eV is about 700 barns, while the cross-section for 0.3 eV neutrons is only 225 barns. Further Thompson estimates that the thermal flux could be as much as 7/6 higher because of leaks in the imprecise Cd shielding (he estimated that only between 75-90% coverage in solid angle was achieved by the shielding). The total estimated uncertainty lies at ±2x.[i]

In April of 2002 NIST reassessed its measurement of the thermal flux in the Low Scatter Room at the request of this project. After further experimentation Thompson determined that the thermal flux in the Low Scatter Room at the time of the USNA TNDS calibration was 1.16 n/cm^2-h with an uncertainty of ±10%.[ii] This calibration is discussed below.

In order to increase the accuracy of the calibration of the low-scatter room, NIST performed a second calibration in April of 2002. In this experiment they used a ^{10}B fission chamber.

From the start, a calibration of the USNA ^{3}He based detector system that was based on boron reactions was considered optimal. Any systematic errors would likely carry over to the ^{3}He detector, since both reaction cross-sections to low energy neutrons are identical, except for a scaling factor. These systematic errors would then be removed from the final evaluation of the environmental neutron fluxes when the calibration constant normalized the measured ^{3}He count rates. That is, if neutrons of 1-100 eV were counted as thermals in the ^{3}He field measurements, these would also be counted in the boron-based calibration. When the field counts were normalized by dividing by the calibration constant, these extra high-energy neutron counts in the field measurements would tend to be minimized. However, boron fission detectors have significant drawbacks: (a) Thin evaporated boron films have poor adherence to many metals, especially the CrO layer on the surface of stainless steel which is normally used. (b) Boron metal has a significantly different thermal expansion coefficient relative to metals. If the boron layer only weakly adheres to its metal substrate, thermal cycles lead to layer flaking. (c) The range of the fission reaction products in metallic boron is far less than 1 μm, while thin boron deposits tend to clump and form hillocks (in part because

of poor adherence), which leads to thick portions in the boron film from which the fission products do not escape, and hence are not measured.

The actual boron layer in the calibration detector was determined by comparing the count rate of the boron deposit to the count rate of a known ^{235}U deposit in a 4.95 Å monochromatic neutron beam according to equation 4-10 below.

$$\frac{\Gamma_U}{\Gamma_B} = \frac{N_U \cdot \sigma_U \cdot \Phi_U}{N_B \cdot \sigma_B \cdot \Phi_B} \qquad \text{(Eq. 4-10)}$$

where Γ is the count rate of the deposit, N is the number of atoms of that deposit, σ is microscopic absorption cross-section of either uranium-235 or boron-10, and Φ is the incident neutron flux. Since the incident flux is the same for both deposits the number of boron atoms (N_B) was obtained according to equation 4-11 below.

$$N_B = \frac{N_U \cdot \sigma_U}{\sigma_B\left(\Gamma_U \big/ \Gamma_B\right)} = 1.29 \times 10^{18} \qquad \text{(Eq. 4-11)}$$

The calibration experiments of the neutron flux in the NIST low scatter room were conducted by Dr. A. Thompson, a NIST scientist. The following discussion is based on his notes. The detector was irradiated in the NIST low scatter room in the same location as the USNA TNDS by a Californium-252 source emitting 1.81×10^8 n/s. A 2000 second background run was performed. The region of interest was defined to be between channels 80 and 512. During the background run, with all sources stored, three counts were registered in the region of interest. During a 3000s data run 1488 counts were registered yielding a count rate (Γ) of .496 s^{-1}.

The absorption cross-section of boron-10 at thermal energy is 3835 barns (that is 3.835×10^{-21} cm^2). The effective target area is the product of the microscopic absorption cross-section and the number of atoms, as calculated in equation 4-12.

$$A_{eff} = N_B \cdot \sigma_B = 1.29 \times 10^{18}\, Atoms \cdot 3.835 \times 10^{-21} cm^2 = 4.947 cm^2 \qquad \text{(Eq. 4-12)}$$

To calculate the thermal equivalent flux and thus the calibration of the low-scatter room we divide the effective target area by the count-rate of the detector as shown in equation 4-13, below.

$$\Phi_{thermal} = \frac{\Gamma}{A_{eff}} = \frac{4.96 \times 10^{-1} s^{-1}}{4.947 \times 10^{-3} cm^2} = 100.26\, s^{-1} cm^2 \qquad \text{(Eq. 4-13)}$$

Since the source used to calibrate the USNA TNDS had a strength of 2.1×10^6 n/s the flux in the low scatter room during the TNDS calibration must be scaled according to equation 4-14.

$$100.26\, s^{-1} cm^2 \cdot \frac{2.1 \times 10^6\, {}^{n}/_{s}}{1.81 \times 10^8\, {}^{n}/_{s}} = 1.16\, s^{-1} cm^2 \qquad \text{(Eq. 4-14)}$$

Then as before the calibration constant was calculated according to equation 4-15.

$$C = \frac{\Phi_{thermal}}{\dot{N}_{bare} - \dot{N}_{shielded}} = \frac{1.16\, {}^{n}/_{cm^2 \cdot s}}{30.2\, {}^{cnts}/_{s} - 2.9\, {}^{cnts}/_{s}} = 0.042\, {}^{n}/_{cm^2 \cdot cnt} \qquad \text{(Eq. 4-15)}$$

The uncertainties surrounding this determination of the thermal flux in the NIST low scatter room are considerably smaller. The several quantities Thompson calculated are shown in equations 4-16 to 4-18.

Fractional statistical uncertainty of the data run:

$$\pm \frac{\sqrt{1488}}{1488} = \pm 0.0259 \qquad \text{(Eq. 4-16)}$$

Fractional uncertainty of the uranium-235 mass used to determine the mass of boron-10:

$$\frac{\pm 1.9\mu g}{191\mu g} = \pm .9.95\times 10^{-3} \qquad \text{(Eq. 4-17)}$$

Fractional uncertainty of the uranium to boron ratio:

$$\frac{\pm 2.2\times 10^{-3}}{6.63\times 10^{-2}} = \pm 3.3\times 10^{-1} \qquad \text{(Eq. 4-18)}$$

The total uncertainty was calculated by adding these quantities in quadrature according to equation 4-19.

$$\sqrt{\left(\pm 2.59\times 10^{-2}\right)^2 + \left(\pm 9.95\times 10^{-3}\right)^2 + \left(\pm 3.3\times 10^{-2}\right)^2} = \pm 4.3\times 10^{-2} \qquad \text{(Eq. 4-19)}$$

Thompson (of NIST) suggested that this 4.3% error might be increased to about 10% because of their experience with systematic errors that have crept into their calibrations in the past. They suggested that a 10% margin of error was adequate to include both random and systematic errors for their calibration experiments. Because of the NIST experience, we have accepted their suggestion of 10% as the calibration error for our thermal neutron detector. [iii]

Calibration in the AFRRI TRIGA Reactor

The Armed Forces Radiobiology Research Institute (AFRRI) is a joint effort between the military services that conducts research in radiobiology. It is located in Bethesda, Maryland. AFRRI operates a 1-megawatt TRIGA (**T**raining, **R**esearch, **I**sotope, **G**eneral **A**tomic) reactor built by General Atomic (see Figure 4-6 and 4-8). It can operate in either pulse or steady state mode. The reactor is equipped with two exposure rooms where samples, equipment, or specimen can be exposed to potentially very large pulses of radiation.[iv]

The USNA TNDS was irradiated in exposure room two (see Figure 4-7) at AFRRI in order to calibrate it to thermal neutrons. Exposure room two is used for experiments that require a high thermal component because it lacks a cadmium-gadolinium shield to the reactor pool (see Figure 4-8). The system was placed inside the exposure room and the data collection PC was connected remotely to the staging area so the system could be controlled from outside the exposure area. Since AFRRI is a high radiation facility, changing the experiment setup in the exposure rooms takes a significant amount of time. Remote control of the system allowed quick transitions between data runs.

The AFRRI exposure room flux was calibrated by the facility utilizing activation analysis. Pure gold foil was exposed to a steady neutron beam from the reactor at a power setting of 100 watts for 20 minutes. One foil was shielded by Cadmium and the other was not. The neutron radiation activates some of the gold in the foil. When the foil is removed from the exposure room the gold molecules that have become radioactive disintegrate and release a photon of known energy. These disintegrations are measured and can be used to calculate a neutron flux. An in-depth discussion of the calculation procedures for activation

analysis is beyond the scope of this report. However, since both AFRRI and NSWC, Carderock, used the foil activation technique to determine the thermal flux, it will be discussed briefly here.

In the foil activation technique a foil of known material is irradiated, and then the gamma emitted is counted. A gamma spectrum with similar characteristics to that shown in figure 3-10 (reaction product spectrum for He-3) is obtained. In foil activation the primary reaction peak is called the gamma photopeak, and is found with the similar pulse analysis electronics as used with the He-3 set-up except the detector has been changed to either sodium iodide or germanium. At AFRRI gold foils were irradiated, while at NSWC Carderock, indium foils were irradiated to determine the flux.

In this technique, the activity is measured by determining the background corrected count rate under the photopeak, from which a saturated activity is determined. The saturated activity of a foil is the theoretical maximum activity (i.e. disintegrations/second) and is based on conditions of an infinite radiation time, zero decay between radiation and counting, no change in activity while counting, and correction for counting efficiency by the gamma detector. When the saturated activity was found at each location, the thermal flux ($n/cm^2 sec$) was then determined by the equation:

$$\Phi_{thermal} = \frac{Saturated\ Activity}{A_{eff}} \qquad \text{(Eq. 4-20)}$$

where the foil effective target area is found similarly to that used in the NIST calibration and given by equation 4-20.

The flux measured by the shielded foil is subtracted from the flux measured by the unshielded foil resulting in the thermal flux for the exposure room at the calibration point for

the given power level. Because the flux is directly proportional to the power level of the reactor, the reactor can provide a variable thermal flux. This experiment was performed twice and the results averaged. At a reactor power setting of 100 watts the calibration location in exposure room two was subject to a thermal flux of 1.55×10^6 n/cm^2-s based on analysis of AFRRI personnel.[v]

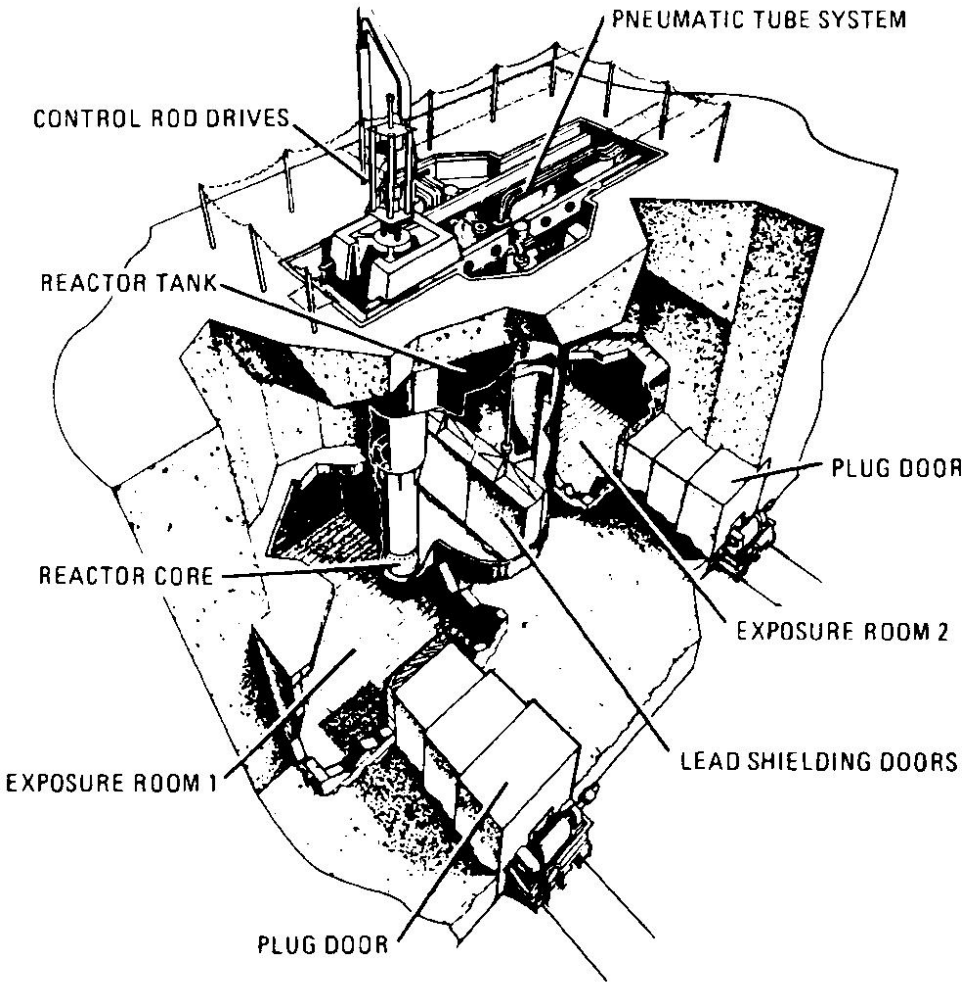

Figure 4-6 Cutaway of TRIGA Reactor

Figure 4-7 USNA TNDS in Exposure room two

Figures 4-6 and 4-7 The TRIGA Reactor at the Armed Forces Radiobiology Research institute was used to calibrate the USNA TNDS. The device was irradiated in exposure room two (see left). The system was controlled remotely from outside the exposure room. The communication cables can be seen in the foreground of Figure 4-3.

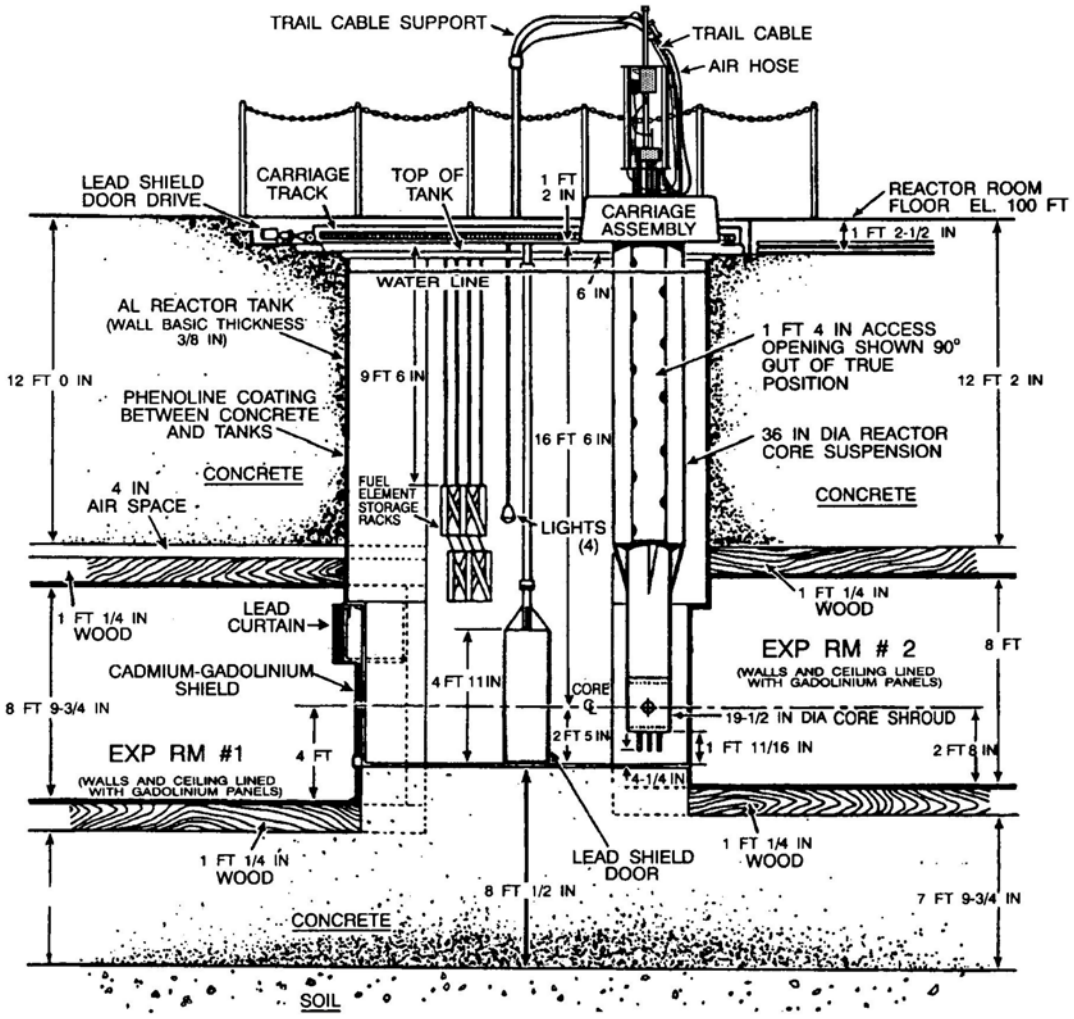

Figure 4-8 AFRRI reactor cross-section showing exposure rooms

Calibration of environmental measurement equipment is difficult with a nuclear reactor. The high flux levels typically associated with a critical reactor tend to swamp the detector system. This was a problem encountered at AFRRI with the USNA TNDS. The first data collection run was performed with the 1-megawatt reactor at 3 mW. At this power setting the reactor is operating in a sub-critical mode. The unshielded tube recorded 448.4 counts per second ($\dot{N}_{bare}$) and the shielded tube recorded 5.45 counts per second ($\dot{N}_{shielded}$). A later data run was performed with the reactor critical at a power setting of 100 mW in which

case the thermal flux was $1.55\times10^{3}\ {}^{n}/_{cm^2\cdot s}$. The shielded tube recorded a count rate of 271.7 counts per second ($\dot{N}_{shielded}$). The unshielded tube was overwhelmed by the large flux, and hence $\dot{N}_{bare}$ could not be accurately determined for this case.

The total neutron flux in the exposure room when the reactor is sub-critical has not been calibrated by AFRRI. Additionally, the low radiation level does not allow activation analysis type calibration. Further, the known calibration cannot be linearly scaled outside of the critical region. However if it is assumed that the ratio, *R*, of thermal to fast neutrons is relatively constant regardless of the criticality of the reactor, a calibration constant (with admittedly large uncertainty) can be obtained. This ratio was found from the count rates observed with the reactor at a power setting of 3mW.

$$R = \frac{\dot{N}_{bare}}{\dot{N}_{shielded}} = 82.1 \qquad \text{(Eq. 4-21)}$$

The product of *R* and the measured shielded count rate for the 100 mW run yields an assumed unshielded count rate notated in equation 4-22 as $\dot{N}_{bare}$.

$$\dot{N}_{bare} = R\cdot\dot{N}_{shielded} = 271.7\ {}^{counts}/_{\sec} = 22366\ {}^{counts}/_{\sec} \quad \text{(Eq. 4-22)}$$

At 100 mW the thermal flux (Φ_2) can be determined by scaling the measured flux (Φ_2) from the 100-watt calibration.

$$\Phi_2 = \Phi_1\cdot\frac{P_2}{P_1} = 1.5\times10^{3}\ {}^{n}/_{cm^2\cdot s} \qquad \text{(Eq. 4-23)}$$

Where P_1 = 100 W and P_2 = 100 mW for the associated fluxes, Φ_1 and Φ_2 in equation 4-23. Referring back to the calibration constant equation 4-2, *C* was then calculated.

$$C = \frac{\Phi_2}{R \cdot \dot{N}_{shielded} - \dot{N}_{shielded}} = \frac{\left(1.56 \times 10^3 \ {}^{n}/_{cm^2 \cdot s}\right)}{22{,}306 - 271.7} = 0.070 \ {}^{n}/_{cm^2 \cdot cnt} \qquad \text{(Eq 4-24)}$$

The Calibration Constant Determined at AFRRI Exposure Room 2

The uncertainty of the calibration constant determined in the AFRRI experiment is significant. The two Au activation experiments performed to determine the flux varied by 17% from the mean. The most significant introduction of error arises from the assumption that *R* is relatively the same for both the critical and sub-critical power settings. This assumption introduces a large error that could not be accurately determined and is roughly estimated from parameters provided by AFRRI personnel as a factor of ±5x. Thus the AFRRI experiment, while not providing a certain calibration constant serves to validate the NIST calibration constant, as the two are within uncertainty of each other. Table 4-2 summarizes the calibration findings for the USNA TNDS.

Facility	Source Type	Flux Calibration Method	$C\left({}^{n}/_{cm^2 \cdot count}\right)$	Uncertainty
NSWC[vi]	Tandem Accelerator	Indium Activation Analysis	0.6	Very Large
NIST	Moderated ^{252}Cf	^{235}U Fission Chamber	0.02	±2x
AFRRI	Nuclear Reactor	Au Activation Analysis	0.07	Large
NIST (APR '02)	Moderated ^{252}Cf	^{10}B Fission Chamber	0.04	±10%

Table 4-2 Summary of Calibrations performed on the USNA TNDS

The AFRRI and most recent NIST calibration are within a factor of two of each other, while the NSWC calibration was viewed as not valid, because of the neutron field orientation. This adds confidence that the calibration constant for the USNA TNDS is correct. The latest NIST calibration run is used for the remainder of this report.

[i] Thompson, Alan K., National Institute of Standards and Technology, private communication.
[ii] Thompson, Alan K., National Institute of Standards and Technology, private communication.
[iii] Thompson, Alan K., National Institute of Standards and Technology, private communication.
[iv] Moore, Mark L., "The TRIGA Reactor Facility at the Armed Forces Radiobiology Research Institute: A Simplified Technical Description," Armed Forces Radiobiology Research Institute, Bethesda MD, 20889-5603
[v] Nguyen, John T., Armed Forces Radiobiology Research Institute, private communication.
[vi] Nelson, Martin, U.S. Naval Academy, private communication.

Chapter 5. Field Measurement Results / Experiments

This chapter discusses the field measurements performed with the USNA Thermal Neutron Detection System and the several experiments that were performed to investigate how the ambient thermal flux was affected by different conditions such as concrete shielding or depth in water.

Beginning in January of 2002 a field survey was begun with the USNA Thermal Neutron Detection System. The primary goal of the survey was to identify any variation in the thermal flux by location with the intention of identifying factors that affected the local terrestrial flux. Measurements were performed in several locations around the Naval Academy grounds, as well as the greater Washington, DC area. The equipment was operated for several hours at each location with the case lid up and connected to 120V AC power. Figure 5-1 shows a distribution of field measurement locations and the measured flux at each location. The one-sigma statistical uncertainty is noted. Table 5-1 on the following page gives a summary description of each field location, and figure 5-2 locates the measurements that were performed on the U.S. Naval Academy.[i] Unlike the large (50-100x) variations that previous terrestrial thermal flux measurements suggested the USNA TNDS measured a relatively constant thermal field of around 5.5 n/cm^2-hr with a standard deviation of 2.5 n/cm^2-hr. Further, the attenuation and shielding effects of local building materials can explain the deviation that was observed. The flux was measured to be highest in offices high above the ground with little material above them (e.g. Field Location 1 and 3). The flux fell off as the detector was placed in locations with more and more building material above it. The lowest flux observed was inside the Naval Academy's neutron generator room. The room is shielded with three feet of high-density concrete and six feet of soil and the flux was a mere 1

n/cm^2-hr (Field Location 5). Buildings composed of low- density materials expectedly showed little effect on the flux. For example, field points 19 and 20 were taken at a house made primarily of low-density materials such as wood. The results show only a small variation when the detector is moved from the upper to the lower floor. Similarly, the flux was only slightly depressed when the detector is moved into the basement of a lightly constructed building. This is to be expected because the number density of atoms in lighter materials is less and thus the probability of an interaction with a thermal neutron is low. Buildings composed of thick concrete decks in contrast show significant thermal neutron attenuation. This observation lead to a series of experiments that are discussed below. When field locations subject to large thermal neutron attenuation (basements, ground floors of large office buildings, etc) are removed from the data set, the average of the fluxes measured at the remaining field locations is 6.3 n/cm^2-hr. The results lead to a conclusion that the unattenuated thermal neutron flux is constant on the order of 6 n/cm^2-hr. Two measurements (at field locations 31, 32) conducted when the atmospheric humidity was 100% (during a rainstorm with no lightning) showed thermal neutron levels twice as high (10.4 n/cm^2-h vs. 5.5 n/cm^2-h) as those measured when there were no rain systems in the area. Although there are confounding factors, such as the barometric pressure shift usually accompanying rain systems, a plausible explanation lies in the moderating effect of water. During a rainstorm caused by a high weather system, there are many thousands of feet of water-saturated air above the ground. Since water is an excellent neutron moderator (see discussion of slowing fast neutrons in Chapter 3) the humidity in the air may account for the elevated thermal flux measured during periods of high atmospheric humidity.

The moderating effect of water was not seen above or near bodies of water as was expected. Measurements (FL 21, 25, 26-28) taken directly over water and in buildings in close proximity to water showed no elevated thermal neutron flux.

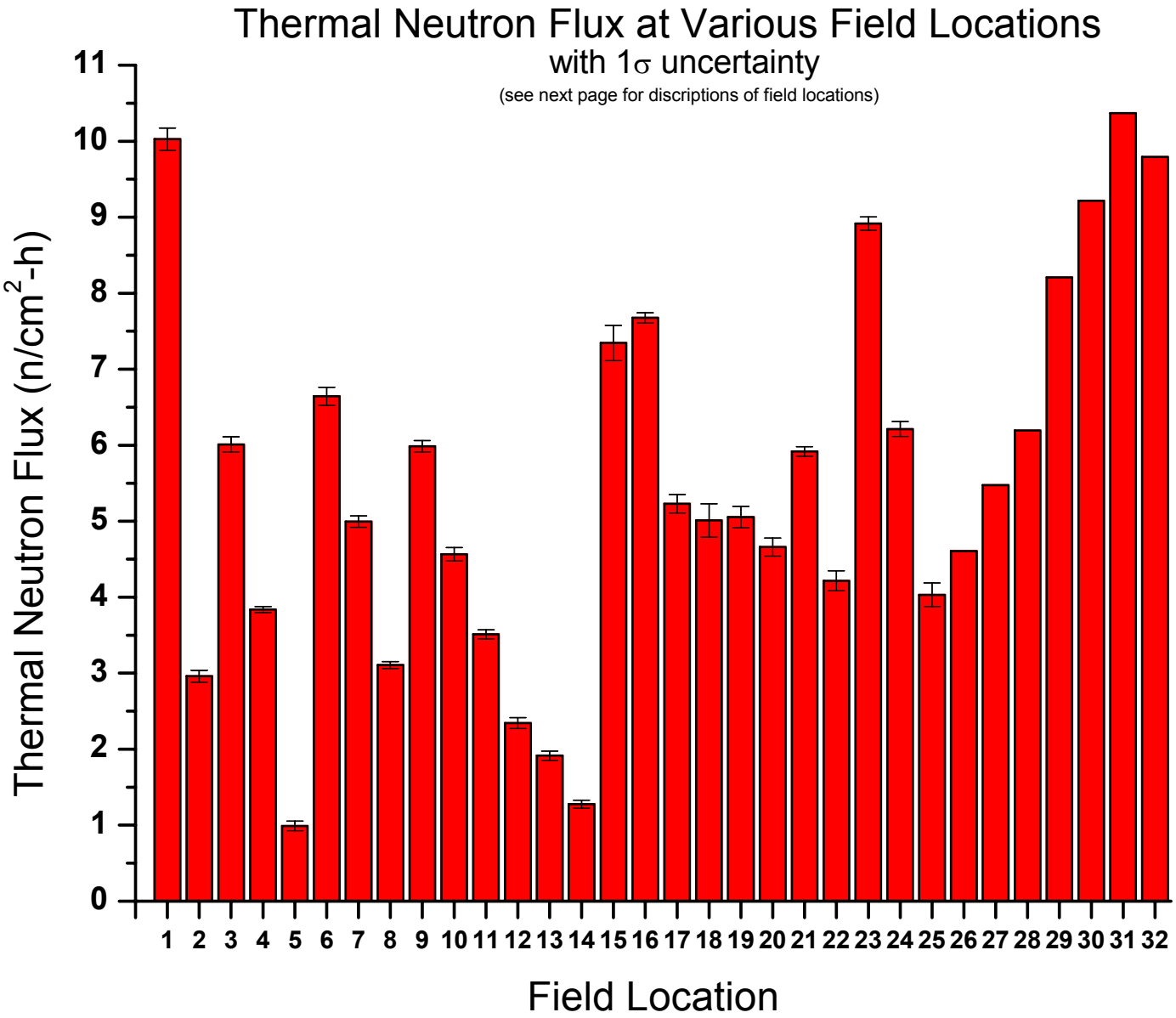

Figure 5-1 Comparison of Thermal Flux measured by the USNA TNDS at various field locations

Field Location Legend		
Ref.	**Location**	**Flux n/cm2h**
1	Rickover 337 4th Floor Office with one wall all windows	10.0
2	Rickover 35c Ground Floor Office with no windows	3.0
3	Michelson 347 4th Floor Office with window	6.0
4	3rd Floor Classroom in center of building - No Windows	3.8
5	Neutron Generator Room - Ground floor Lab with 3 feet high density concrete and 6 feet soil overhead	1.0
6	Mahan Crossover 3deck - 3rd Floor hallway/ windows both sides	6.6
7	Mahan Crossover 2deck - 2nd Floor hallway/ windows both sides	5.0
8	Mahan Crossover Ground - 1st Floor hallway/ windows one side	3.1
9	Bancroft Deck 1-4 Granite Midshipmen Dormitory Top Floor	6.0
10	Bancroft Deck 1-3 Granite Midshipmen Dormitory 4th Floor	4.6
11	Bancroft Deck 1-2 Granite Midshipmen Dormitory 3rd Floor	3.5
12	Bancroft Deck 1-1 Granite Midshipmen Dormitory 2nd Floor	2.3
13	Bancroft Deck 1-0 Granite Midshipmen Dormitory 1st Floor	1.9
14	Bancroft Basement	1.3
15	Residence Basement Greater Annapolis	7.3
16	Residence in Rural MD / light building materials	7.7
17	Annapolis, 1st floor / light building materials	5.2
18	Annapolis, 2nd Floor	5.0
19	Condominium Arlington, VA, 2nd Floor / light building materials	5.1
20	Condominium Arlington, VA, Basement	4.7
21	Hendrex Oceanography Lab / wood steal construction, surrounded on 3 sides by water	5.9
22	Smoke Hall - Large Hall with granite walls and windows	4.2
23	Residence Davidsonville, MD, 2nd Floor, light building materials	8.9
24	Bancroft Deck 1-4 (Different Location)	6.2
25	Wood Boat Dock, one meter above water	4.0
26	House, 1st floor in 1 story wood house. with wood roof, 150' from water. Edgewater MD	4.6
27	House, 1st floor in 1 story wood house, with wood roof, 150' from water. Edgewater MD (different loc.)	5.5
28	House, 1st floor in 2 story wood house, with wood roof, 150' from water. Edgewater MD	6.2
29	House, Basement under 2 story wood house, 150' from water. Edgewater MD	8.2
30	Repeat of above #29	9.2
31	During constant RAIN, no lightning, 100% humidity. Same location as #27 above.	10.4
32	Repeat of #31. Rain slowly subsided. 12 hour run. Same location as #27 above.	9.8

Table 5-1 Summary of Field Measurements

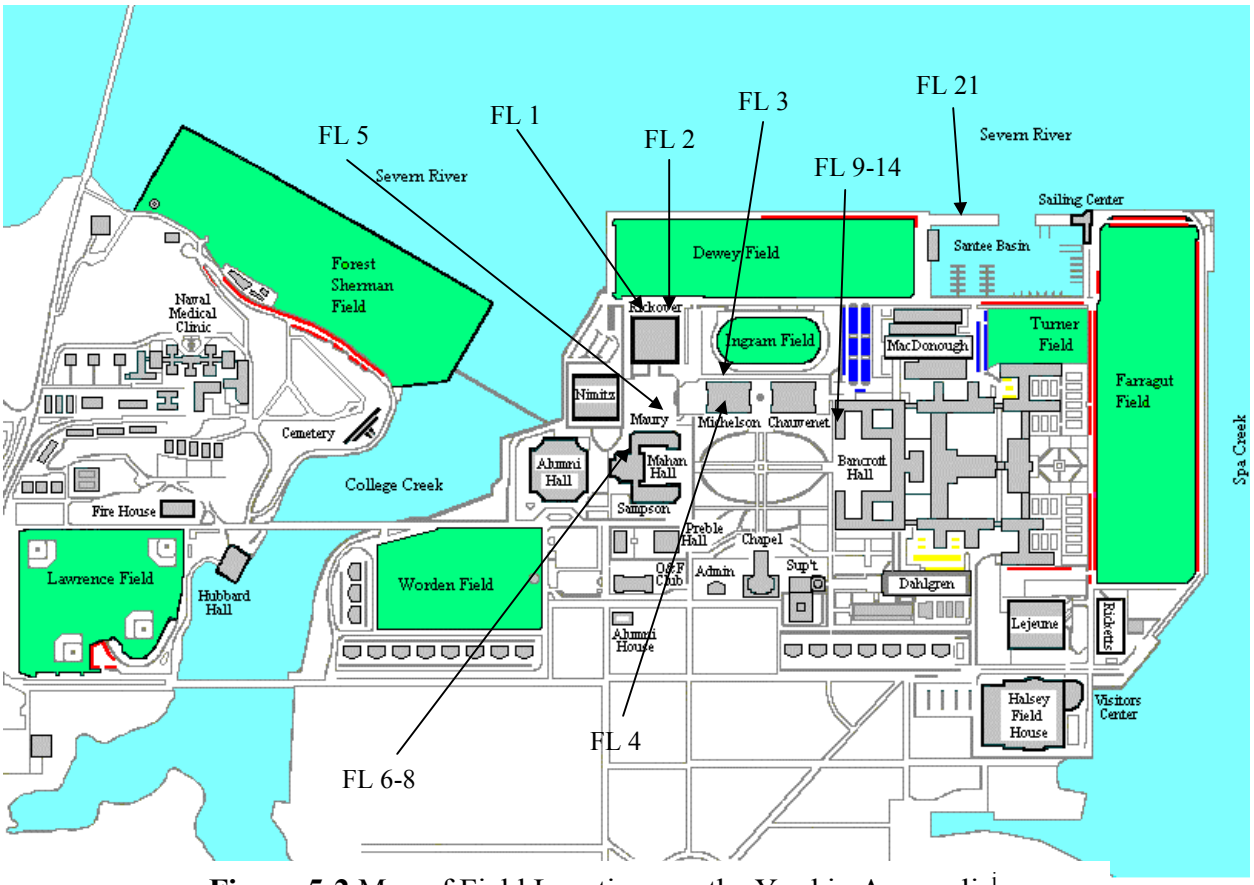

Figure 5-2 Map of Field Locations on the Yard in Annapolis[i]

Attenuation Experiments

Electronic systems are usually within buildings, shielded by concrete or other structural materials from cosmic rays. Also, there is the special case of electronics in submarines that are shielded by seawater. In order to evaluate the neutron flux in these places, experiments were conducted to measure the attenuation of cosmic ray thermal neutrons under shielding by concrete and seawater.

In order to investigate the attenuation effect of building materials on the thermal flux, several experiments were performed. In the first, the USNA TNDS was placed

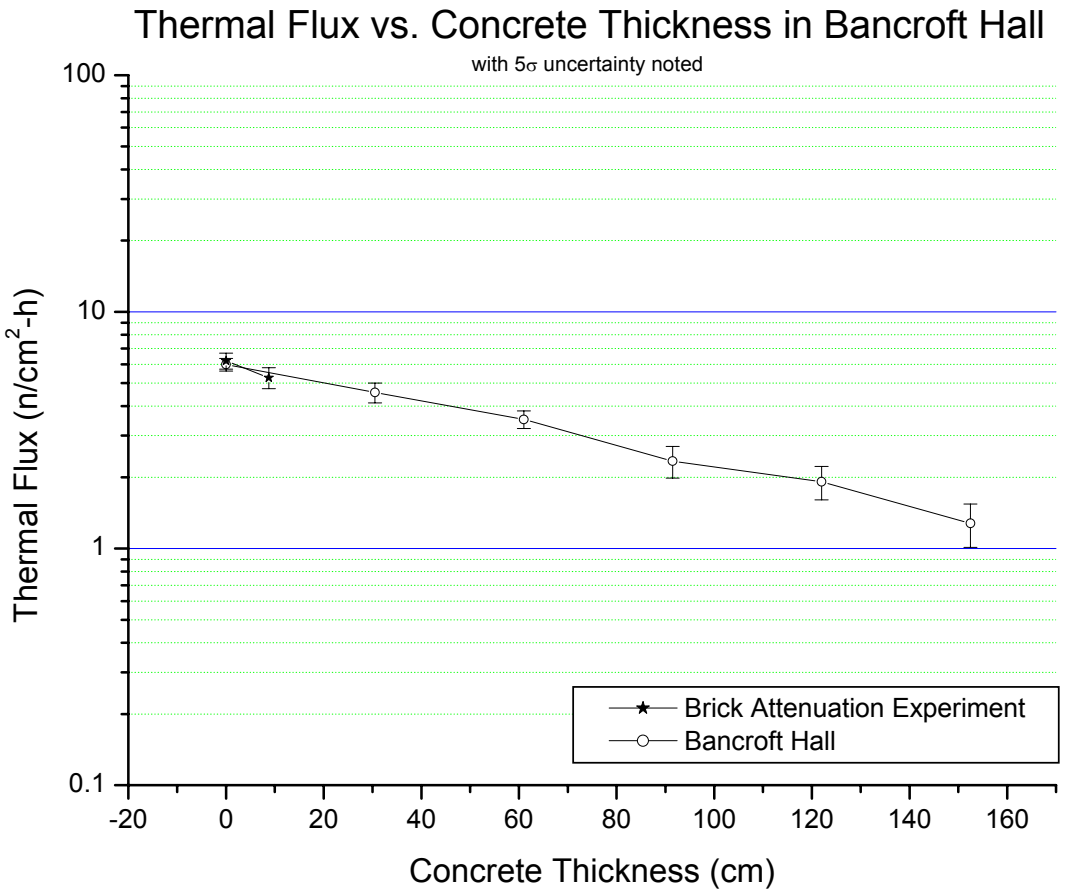

Figure 5-3 Thermal flux vs. thickness of concrete above the detector in Bancroft hall.
Note: The brick attenuation experiment was conducted with brick on all sides of the detector.

on the several floors of the Midshipman dormitory, Bancroft Hall. Bancroft Hall is a 5 story concrete and granite building. Each subsequent measurement was taken on a lower floor, thus increasing the amount of concrete above the detectors. The measured flux fell from 6.0 n/cm^2-h to 1.3 n/cm^2-h between the top and bottom decks. Figure 5-3 shows how the flux varied with the amount of concrete above the detector. With each additional deck above the detector, the thermal flux decreased logarithmically (see figure 5-3). A second experiment was performed on the Yard with the same intent (field locations 6-8 in figure 5-2). This time the detector was placed on each of three levels of a concrete and granite crossover connecting Mahan and Maury halls. The crossover is lined with large windows on the upper two decks. Figure 5-4 shows how the flux varied with floor on the crossover.

The attenuation of cosmic rays is usually considered using the formalism of linear cascade theory in which the major cross-sections of both creation and absorption are smoothly changing with hadron energy. These assumptions are assumed to hold for low energy neutrons. In this case, the change of intensity with shielding depth can be expressed as:

$$I(x) = I_o e^{-x/u} \quad \text{(Eq. 5-1)}$$

where I is the particle flux under shielding of depth x (usually expressed as g/cm^2) is equal to the unshielded flux, I_o, time the exponential factor of -x/u, where u is the mean attenuation coefficient, also expressed in g/cm^2. Note that x is the shielding depth times the mean density of the material.

Portland cement concrete nominally is a 1:2 mix of cement and sand, which contains 10% water by weight. This approximates nominal building standards for commercial structures in the Unites States. Concrete densities may vary by up to 20%, especially if

aggregate is included, so any concrete absorption calculation will be a rough estimate unless the details of the material are known. The attenuation of cosmic ray neutrons has been studied for neutrons of energies of 0-10 MeV by Yamashita et al in 1966[ii]. These authors used a 6 story, parking garage to obtain shielding measurements for a low-energy neutron detector. They obtained a mean attenuation coefficient of 170 g/cm^2. They did not analyze the concrete of the garage, so the error of their measurement by this one factor would scale with the known densities of commercial concrete: 2.3 - 2.75 g/cm^3. This would mean that values of 150 - 190 g/cm^2 would be possible depending on the grade of concrete.

A more extensive set of experiments was reported for high-energy cosmic ray neutrons, with energies above 50 MeV by Ziegler in 1996.[iii] Ziegler's group found very consistent results under various depths of natural limestone, with a mean attenuation coefficient of 155 g/cm^2. The Ziegler paper set a mean error of 2% of this result.

Figure 5-5 shows both the results of Ziegler (above), noted as "High Energy Neutrons," and this project's results in Bancroft Hall noted as "Thermal Neutrons." In this plot both flux results have been normalized to unity at zero concrete depth. The Bancroft hall data yielded a deep-shielding attenuation coefficient of 102 g/cm^2, in disagreement with the value of 155 g/cm^2 of Ziegler. The explanation of the large attenuation for light shielding may be caused by the distribution of the flux of incident cosmic rays. The incident neutron flux as a function of zenith solid angle has been studied by many authors and is reviewed in the Ziegler article (above). The mean value is that the flux decreases by the cos^2 of the zenith angle of its incident trajectory. The attenuation of this flux is non-linear (exponential) so the attenuation of neutrons coming from angles of 45 degrees from the apex is far higher than those from directly above. Added to this is the complication of attenuation by vertical walls

within Bancroft. These will further attenuate the low-angle neutrons while having little effect on the vertically incident neutrons. Hence, the first 80 g/cm^2 of concrete can be said to be efficiently screening out the high-angle neutrons, leaving the vertical flux. By the time measurements were being conducted on Deck 3 of Bancroft, only the vertical trajectory neutrons were significant. Hence, the basis of the mean attenuation coefficient of 102 g/cm^2 may be argued as an accurate attenuation of neutrons by concrete since it applies only after the incident neutrons have become collinear. The experiments discussed above were not analyzed to take into account the non-linear absorption of cosmic rays as a function of their direction, so their values were considerably higher.

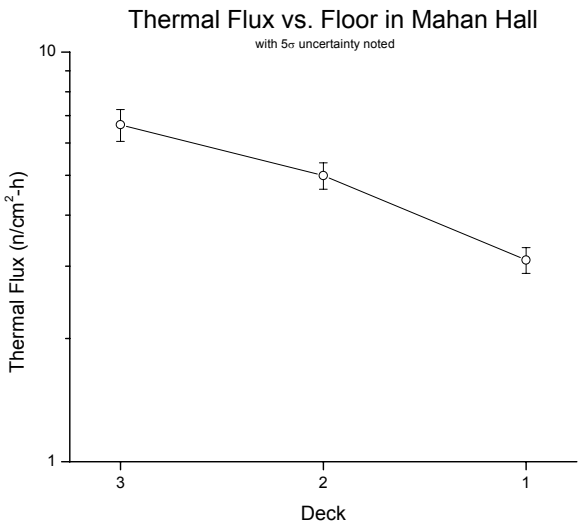

Figure 5-4 $\Phi_{thermal}$ vs. Deck of Mahan Crossover

When compared to the attenuation of high-energy neutrons, the thermal neutron flux seemed to attenuated more quickly (see figure 5-5). While the two experiments using multi-floored attenuation suggested that the thermal flux was more quickly attenuated, too many confounding factors existed. It is difficult to know how consistently thick the shielding is above the detector, or whether the makeup of the concrete is homogeneous. To broaden this observation a third experiment was performed using water.

The USNA TNDS was equipped with a twenty foot SHV cable. The unshielded detector was then lowered into a five-meter long PVC pipe that was submerged in

water and exposed to the open air. Figure 5-6 illustrates the results of this experiment. For both data sets the attenuation of the thermal flux was plotted with the attenuation of high-energy neutrons observed by Ziegler of IBM. In both cases, the thermal flux falls off more quickly. The attenuation of neutrons by water has also been studied once before (see Ziegler above). This experiment gave a mean attenuation coefficient of 210 g/cm^2 for high-energy neutrons (> 50 MeV). The USNA experiment was conducted in the Chesapeake with a mean salt-water temperature of 12^{o}C. This experiment could only be conducted to a depth of 220 cm because of equipment limitations. The attenuation showed an immediate drop-off of thermal neutrons, and then a steady attenuation with depth with a mean attenuation coefficient of 200 g/cm^2. The initial drop-off was an experimental anomaly since the detector was 18 cm long, and hence measured thermal neutrons over a significant portion of the shallowest depth (47 cm). There is the additional factor that water is the most efficient moderator of energetic neutrons (see more discussion in chapter 3). This means that for the shallowest depths (<100cm) there is a large conversion of energetic neutrons to thermal energies. Below this depth, the attenuation becomes more like a linear cascade and stabilizes at 200 g/cm^2. Thus it is reasonable that the initial meter of seawater acts to moderate and absorb medium energy neutrons, and below this the thermal neutron flux attenuates with a steady coefficient of 200 g/cm^2.

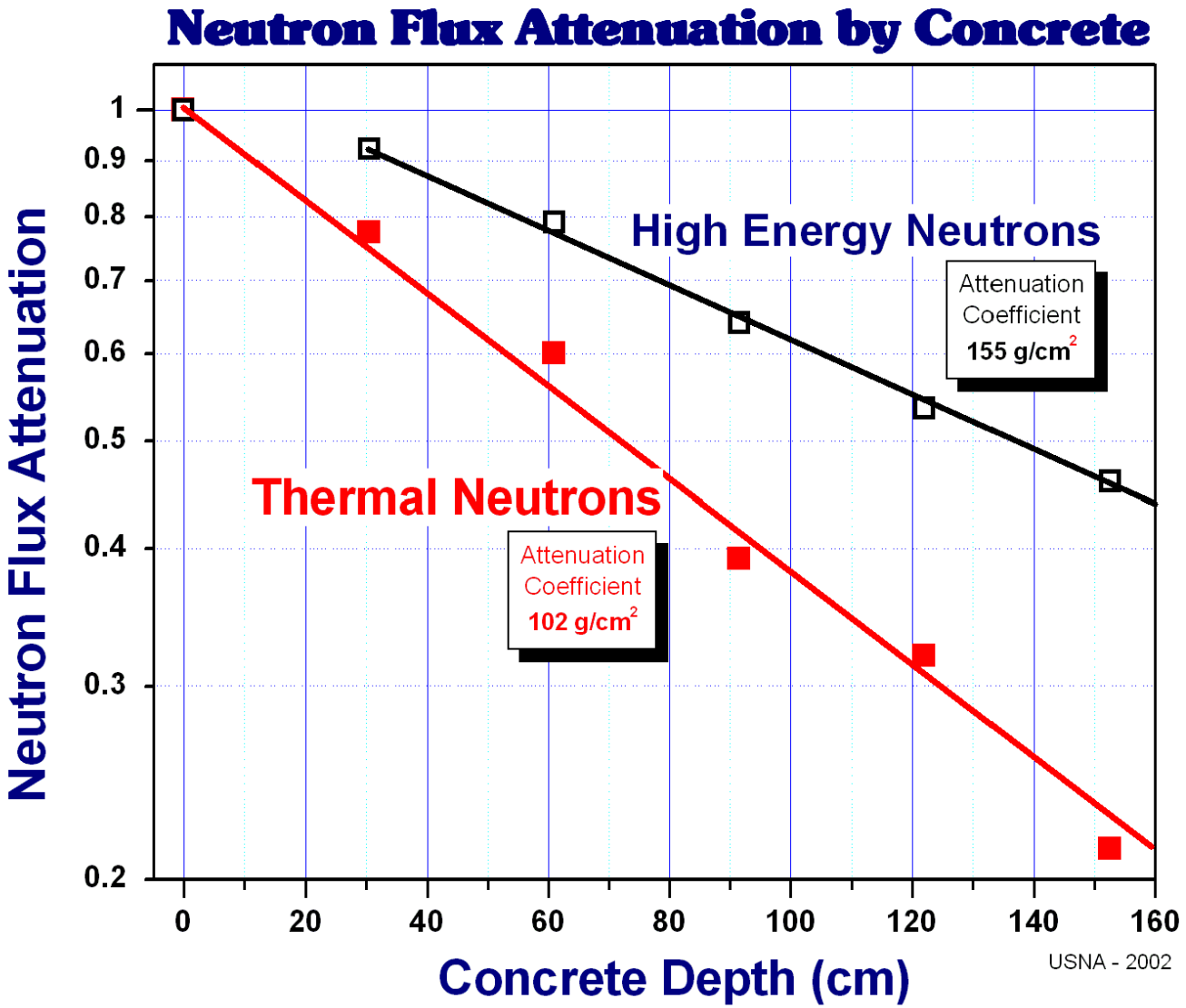

Figure 5-5 Neutron Flux attenuation by Concrete

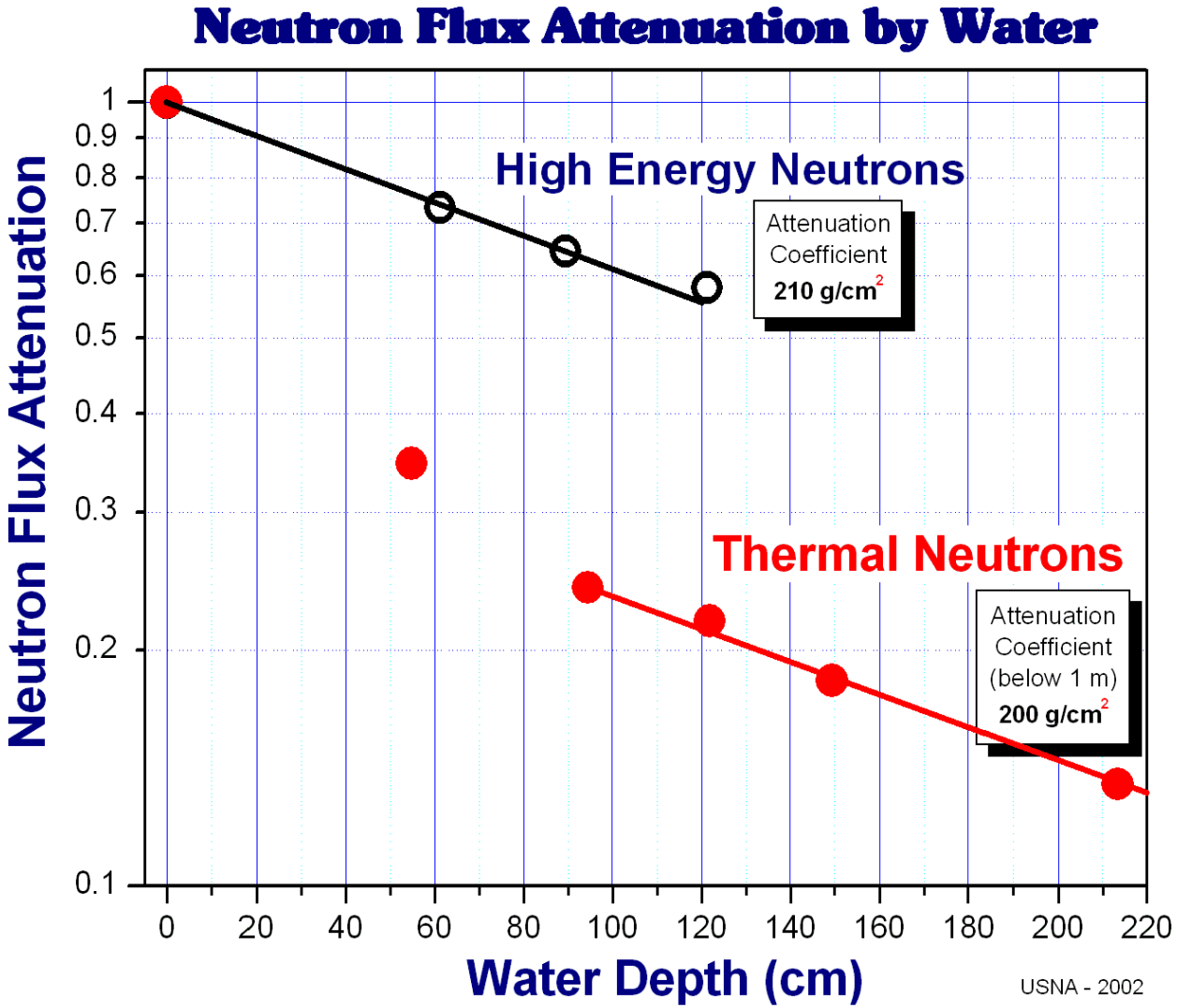

Figure 5-6 Neutron flux attenuation by water

The final experiment performed with the USNA TNDS into building material effect on the thermal flux was to surround the detectors in concrete or polyethylene and observe the effect. The three-foot SHV cable was returned to service and data was taken on the top floor of Bancroft Hall. The control measurement recorded a thermal flux of 6.21n/cm^2-h. Then the two helium-3 probes were surrounded by 8.75 cm of concrete blocks. The TNDS measured an attenuated flux of 5.27n/cm^2-h. These data points are compared to the building based measurements in figure 5-4. The TNDS was then surrounded by 2.5 cm of polyethylene. The flux measured by the TNDS was 10.3 n/cm^2-h. When materials populated by lighter atoms, such as polyethylene or wood, surround the detector the thermal flux is elevated by the moderating effect of the surrounding material. When more and heavier material surrounds the detector, the thermal flux is depressed by the shielding of the material.

Electronic Reliability

The impetus for this project was the soft errors that ambient thermal neutrons cause. The results of the measurements of the USNA Thermal Neutron Detection System in terms of single event upsets (SEUs) is discussed in this section.

The SEU cross-section of a microelectronic device is the probability of a fail given the flux and the size of the chip. The SEU cross-section has units of (cm^2 fails)/bit. The product of the thermal flux (Φ), the SEU cross-section (χ), and the chip size (N_{bits}) is the SEU rate represented by the symbol λ (units of fails/hour), where the chip size is measured in bits and is found by equation 5-2 as:

$$\lambda = \Phi \cdot \chi \cdot N_{BITS} \qquad \text{(Eq. 5-2)}$$

The reciprocal of λ is the mean time to failure (*MTF*), which can be calculated by equation 5-3.

$$MTF = \frac{1}{\Phi \cdot \chi \cdot N_{BITS}} \qquad \text{(Eq. 5-3)}$$

Using SEU cross-section data for several commercial DRAM devices measured at the NIST thermal column,[iv] an example mean time to failure was calculated. Table 5-2 shows three devices labeled A, B, C (manufacture and model numbers have been withheld), their SEU Cross Section, the SEU rate in a 100 gigabyte (GB) system and the mean time to failure for a 100 GB system. The SEU rate calculation for device A is shown in equation 5-4.

$$MTF = \left(5.5\,{}^{n}\!/_{cm^2 \cdot h}\right) \cdot \left(4.3 \times 10^{-16}\ {}^{fails \cdot cm^2}\!/_{bit}\right) \cdot \left(8 \times 10^{11}\, bits\right) = 1.1 \times 10^{-3}\ \frac{fails}{hour} \qquad \text{(Eq. 5-4)}$$

Table 5-2 shows that in such a system would have a mean time to failure (λ) of 21.9 days. Each time a major banking or communication system crashes the manufacturer sends out representatives to correct the problem. Even if the error was a non-permanent soft-fail, equipment is often replaced and the cost to the manufacturer to honor service agreements can be many tens of thousands of dollars per fail. The expenses associated with such soft fails are what prompted support for this research.[v]

Device	Thermal SEU Cross-Section[ii] χ (cm^2 fails)/bit	SEU Rate in 100 GB system λ ($hours^{-1}$)	Mean time to failure *MTF* (days)
A	0.43	1.9×10^{-3}	21.9
B	0.22	9.7×10^{-4}	43.0
C	0.0022	9.7×10^{-6}	4303.4

Table 5-2 SEU Characteristics of Several Undisclosed SRAMs

The field measurement survey by the USNA TNDS yielded several interesting results. First, the high variability of the thermal flux over small changes in location the project sought

to observe was not seen. Second, the thermal flux is more quickly attenuated by building materials than is the higher energy cosmic ray induced neutron flux. The variations that do exist in the local ambient flux are primarily due to shielding. That is to say that the more material above the field location, the lower the flux. The exception is that a small amount of material surrounding the field location will actually increase the thermal flux by moderating faster neutrons present in the environment. Lastly, the USNA measurements have been represented in real world failure predictions for modern microelectronic devices.

[i] Map from USNA official website www.usna.edu/Performance.
[ii] M. Yamashita, L. D. Stephens and H. W. Patterson, J. Geophys. Res., 71, 3817 (1966)
[iii] J. F. Ziegler, IBM J. Res. and Dev., 40, 19 (1996)
[iv] Ziegler, J., Private Communication.
[v] Ziegler, J., Private Communication.

Chapter 6. Conclusions and Recommendations

Conclusions

After one year of work the USNA Thermal Neutron measurement project has produced a NIST calibrated, portable, and reliable system for the measurement of the thermal neutron flux at background intensities. A survey of various field locations was conducted. This project concluded that the previously reported thermal flux measurements that showed very large variations (up to 50x) are not substantiated by the USNA measurements. The variations in the flux that were observed were determined to be due to the shielding effect of local building materials. The unattenuated ambient terrestrial thermal flux around the USNA was determined to be in the range of 3.9 to 9.9 n/cm^2-h, a variation of about 2x. An attenuated thermal flux was observed to vary by a factor of 4.6x between the 4th deck and the basement of Bancroft Hall, and by a factor of 2.1x between the top (3rd) and ground floors of the Mahan crossover. It was determined that the cosmic ray induced thermal flux is attenuated more quickly than the cosmic ray induced fast neutron flux. In concrete it was found the cosmic ray induced thermal neutron flux had an attenuation coefficient of 102 g/cm^2 which is less than the 155 g/cm^2 measured by Ziegler for cosmic ray induced fast neutrons. Similarly, in water this project calculated a neutron attenuation coefficient of 200 g/cm^2, which is approximately the same as Ziegler's 210 g/cm^2 for high energy neutrons.

This project found that the BC-702 Scintillation type thermal neutron detector was not useful in a mixed field due to its high sensitivity to gamma rays. This sensitivity precluded its calibration in any mixed field and thus its use in this project.

Based on the ambient flux measurements made by the USNA TNDS the mean time to failure for three commercial microelectronic devices was calculated at 22, 43, and $3.3x10^3$ days (for 100GB system).

One of the principle successes of this project was the calibration of the USNA Thermal Neutron Detection System. When the project began, several government laboratories indicated that they could calibrate the USNA TNDS with their standard thermal neutron setup, since they used thermal neutrons in a variety of physical and engineering experiments and applications. Three different government facilities (two military and NIST), however, had difficulty providing an accurate calibration. They initially differed from each other by several orders of magnitude. The original calibration flux reported by NIST was 7 n/cm^2-s. After recalibrating their low-scatter room, the same flux level was reported as 16 times smaller ($4.4x10^{-1}$ n/cm^2-s), which was later readjusted to $5.5x10^{-1}$ n/cm^2-s. Recently (APR 2002) with another, more complex, experiment, they revised their measurement of the same flux to 1.16 n/cm^2-s. The uncertainty fell over the course of the calibration from ±2x to an acceptably low ±10%. The other two facilities were unable to ascertain an uncertainty for the neutron fields used to attempt calibration. Thus the USNA currently possesses the only thermal neutron detection system with an accurate NIST traceable calibration.

Recommendations

The most important result of this research has been the attainment of a reliable and calibrated thermal neutron detection system. The "nuclear Navy" depends on accurate measurements of thermal neutrons as part of their protocols in establishing personnel safety. The difficulty that established United States laboratories had in providing a cross-checked neutron flux raises serous questions about instrumental calibrations. The standard detector to

measure thermal neutrons in the US Navy today at sea and in shore facilities is the AN/PDR-70. The output of this instrument is given in mrem/hr. However, the thermal flux in a location can be determined from this instrument by using the known dose rate to thermal flux conversion factor of 260 n/cm^2-s equals 1 mrem/hr[i] and taking two measurements as done in this project -one with the AN/PDR 70 bare and the other with it shielded either with cadmium or borated silicate. Hence, it is recommended that the USNA calibrated detection system be taken to a shipboard environment and the two systems be compared against each other.

Further study into the thermal flux should investigate if the increase in the thermal flux observed during times of high atmospheric humidity is a real effect, or if it is due to some other, hereto unknown, factor. Now that the TNDS is functional, a larger survey of should be conducted of terrestrial and low altitude field locations. The TNDS should be flown in an aircraft and the thermal flux measured as a function of altitude. More attenuation experiments should be performed with more data points to determine more exactly the form of the thermal flux attenuation. Specifically, measurements should be conducted at sites of microelectronics vendors where SEU problems have been observed. Additional calibrations should be performed on the USNA TNDS at the thermal column of the NIST reactor.

Lastly an extensive survey of open-air sites should be conducted in the warm months to determine more precisely what the unattenuated thermal flux is. This survey could not be conducted during the course of this project because the cold weather affects the consistency of the preamplifiers. Understanding the natural thermal neutron environment more is imperative to both the electronic reliability issue and perhaps to nuclear arms control and proliferation.[ii]

[i] ICRP Publication 21, Radiation Quantities and Units, Appendix 6, 1971

[ii] USNA is currently investigating the detection of highly enriched uranium (HEU) for the Defense Threat Reduction Agency (DTRA) using neutron stimulation. Ambient thermal neutrons could be a potential source of this stimulation.

Bibliography

Baumann, R. C. Texas Instruments Co. private communication.

Baumann R. C., T. Z. Hossain, E. Smith, S. Murata and H. Kitagawa, "Boron as a primary source of radiation in high density DRAMs." *IEEE 33rd Annual Intnl Reliability Physics Proc.* p297-302, 1995.

Baumann R. C., T. Z. Hossain. S. Murata, H. Kitagawa. "Boron Compounds as a Dominant Source of Alpha Particles in Semiconductor Devices." IEEE Proc. IRPS, p.297, 1995.

Baumann R. C. and E. B. Smith. "Neutron-induced ^{10}B fission as a major source of soft errors in high density SRAMs." *Microelectronics Reliability.* vol. **41**, no. 2, p.211, 2001.

Baumann R. C. and E. B. Smith. "Neutron-Induced Boron Fission as a Major Source of Soft Errors in Deep Submicron SRAM Devices." IEEE Proc. IRPS, p. 297, 2000.

Baumann R. C. "Soft Error Characterization and Modeling Methodologies at Texas Instruments." Semiconductor Research Council 4th Topical Conf. On Reliability. SemaTech CD-ROM 0043-3283, 2000.

"BC-702 Thermal Neutron Detector." Bicron. Available online http://www.bicron.com/bc702.htm (APR 2002).

DOE/ER-0457T. U. S. NIM Committee May 1990. Report available as "Standard NIM Instrumentation System." NTIS. U. S. Department of Commerce. Springfiled. VA, 22161.

Heusser, G. "The Background Components of Germanium Low-Level Spectrometers." Nucl. Inst. and Methods, **B17**, p418-422, 1986.

IBM Journal of Research and Development, vol. **40**, 1996.

Knoll, G. *Radiation Detection and Measurement*. 3rd Edition. New York: John Wiley & Sons, Inc.

Korean Atomic Energy Research Institute Online at http://hpngp01.kaeri.re.kr/CoN/endfplot.shtml. (APR 2002)

Moore, Mark L. "The TRIGA Reactor Facility at the Armed Forces Radiobiology Research Institute: A Simplified Technical Description." Armed Forces Radiobiology Research Institute. Bethesda MD. 20889-5603.

Nelson, Martin. U.S. Naval Academy. private communication.

Nguyen, John T. Armed Forces Radiobiology Research Institute. private communication.

O'Brien K., H. A. Sandmeier, G. E. Hansen and J. E. Campbell. J. Geophys. Res. p**83**, p114, 1978.

"Radiation Quantities and Units." ICRP Publication 21. Appendix 6. 1971.

Sarlese, J. A. "Development of a Semi-Empirical Model for SEUs in Modern DRAMs." Trident Scholar Project Report: no. 277. U.S. Naval Academy, May 2000.

"Signal Processing Electronics." EGG-Ortec Electronics Catalog, 2001. also available online at http://www.ortec-online.com.

Thompson, Alan K. National Institute of Standards and Technology. private communication.

USNA official website. Available online: http://www.usna.edu/Performance (APR 2002).

Wolf, S. and R. N. Tauber. "*Silicon Processing for the VLSI Era.*" Lattice Press, p.86. 1986.

Yamashita M. Stephens L. D. and Patterson H. W. J. Geophys. Res. p71, 3817. 1966.

Zabel T. IBM-Research. private communication.

Ziegler J. F. IBM J. Res. and Dev. p40, 19. 1996.

Ziegler, J. F. United States Naval Academy. private communication.

APPENDIX A BC-702 Scintillation Detector

BC-702
Thermal Neutron Detector
General Description

BC-702 is a highly efficient scintillation detector of thermal neutrons which provides excellent discrimination against gamma background. The detector is a disc 0.25" (6.35mm) thick available in several diameters which can be mounted directly to photomultiplier tubes or light guides and surrounded by an appropriate moderator.

The thermal neutron detector incorporates a matrix of a lithium compound enriched to 95% ^{6}Li dispersed in a fine ZnS(Ag) phosphor powder. The detection process employs the nuclear reaction ^{6}Li (n, α) ^{3}H in which the resulting alpha particle and triton produce scintillations upon interacting with the ZnS(Ag). The BC-702 thermal neutron detector is an improved version of that developed by Stedman[1] with the scintillating portion of the detector being convoluted to maximize light output.

Performance Characteristics

The thermal neutron detector efficiency varies with neutron energy as the following approximate values indicate.

Neutron Energy	Efficiency
0.01 eV	60%
0.025 eV	55%
0.1 eV	30%
1 eV	10%

In most applications, the BC-702 will give counting efficiencies up to twice those possible with similar detectors based on ^{10}B. The neutron detection efficiency attainable in a specific application will depend on the level of the gamma ray background.

Gamma discrimination can be achieved to enable efficiency detection of thermal neutron fluxes in gamma fields as high as 10 R/hr (10^{7} gamma rays per neutron). In lower gamma fields (<100 mR/hr) discrimination is easily achieved by setting a lower threshold. In fields above 1R/hr, several gamma interactions occurring within the

resolving time of the detector could produce a composite pulse as large as that from a neutron. in this case, pulse shape discrimination may be effectively used.

Properties

Lithium Content	11mg/cm^2
Wavelength of maximum emission	461 nm
Light Output	Pulses up to a maximum of ZnS(Ag) (comparable to NaI(Tl))
Decay Time	0.2 microseconds

Standard Sizes

Size	**1"**	**1.5"**	**2"**	**3"**	**5"**
Overall Diameter	1"	1.5"	2"	3"	5"
Overall Diameter	25.4mm	38.1mm	50.8mm	76.2mm	127.0mm
Sensitive Area (dia)	22.2mm	34.9mm	47.6mm	73.0mm	123.8mm
Sensitive Area (cm^2)	3.8	9.5	17.8	41.8	120.4

Reference

1. R. Stedman, Rev. Sci. Instr., 31, 1156 (1956)

Discussion and tables provided by Bicron who manufactures this product.

APPENDIX B

Additional Neutron Cross Section Plots and Material Composition Information

This appendix contains the cross section plots (figures B-2 – B-10) of important isotopes found in materials used in this project. Also given in this appendix is the mass fraction composition of the Borated Silicate (figure B-1), which was used in this project as a thermal neutron shield. The first four plots (figures B-2 – B-5) show the neutron total cross-sections for materials used in neutron detectors namely: lithium-6, uranium-235, cadmium, and helium-3. The following four plots (figures B-6 – B-9) show the neutron total cross-sections for isotopes commonly found in buildings, the environment, and detector housings: carbon, hydrogen, oxygen, and iron. The last cross-section plot is that of Boron-10 (figure B-10), which was used in for shielding.

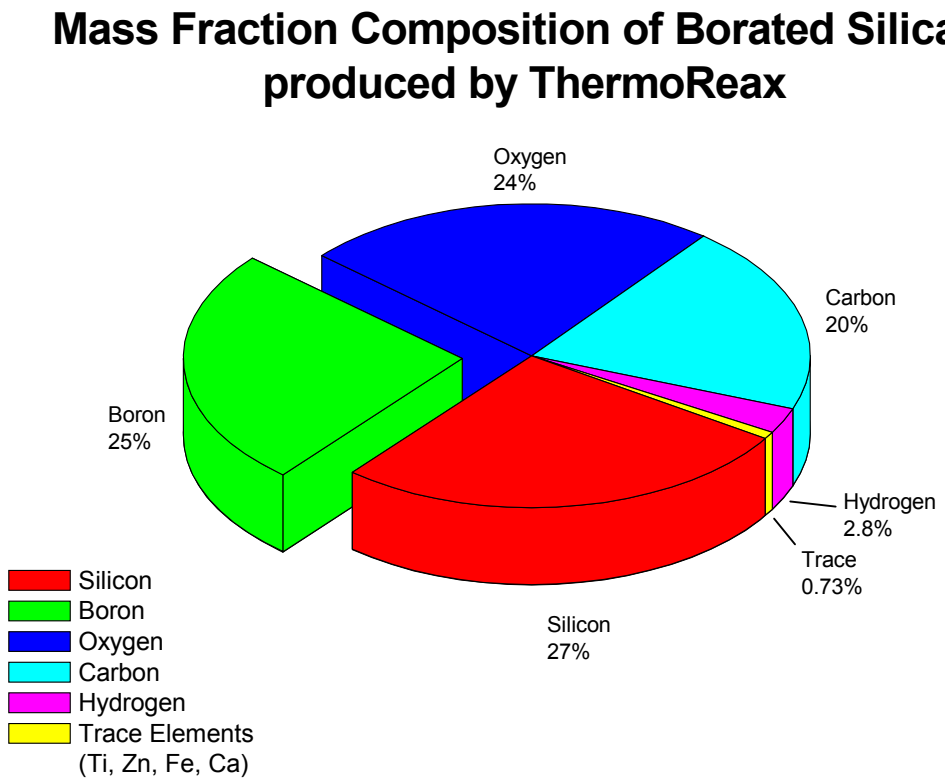

Figure B-1 Composition of borated silicate used as a thermal neutron shield in the USNA TNDS Information provided by the manufacturer: ThermoReax

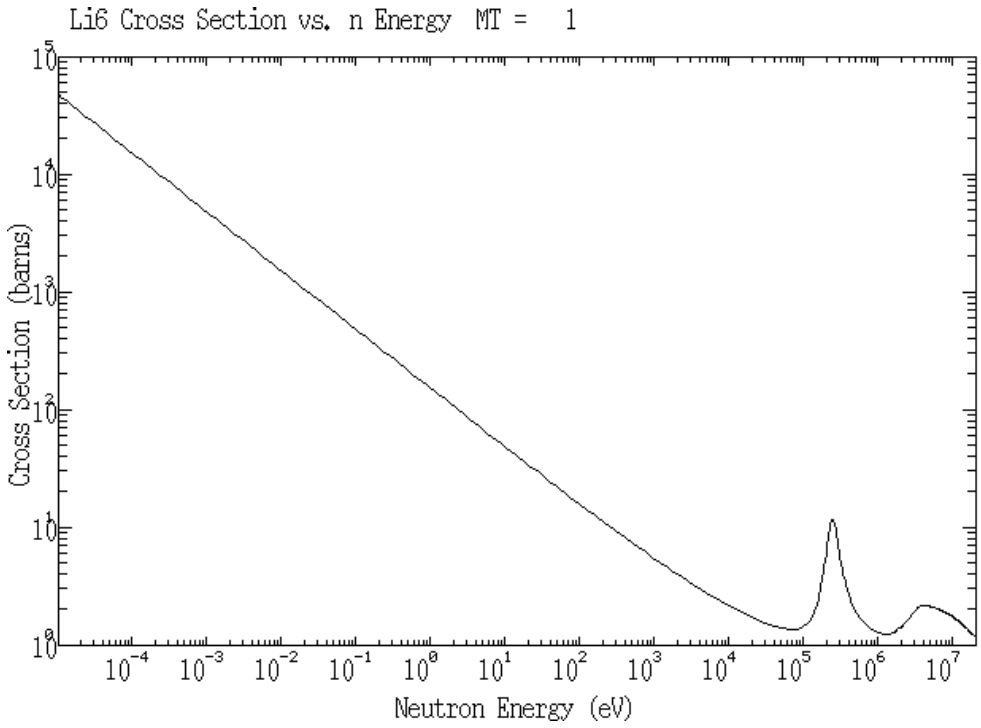

Figure B-2 Cross-section of Li-6 vs. neutron energy[i]

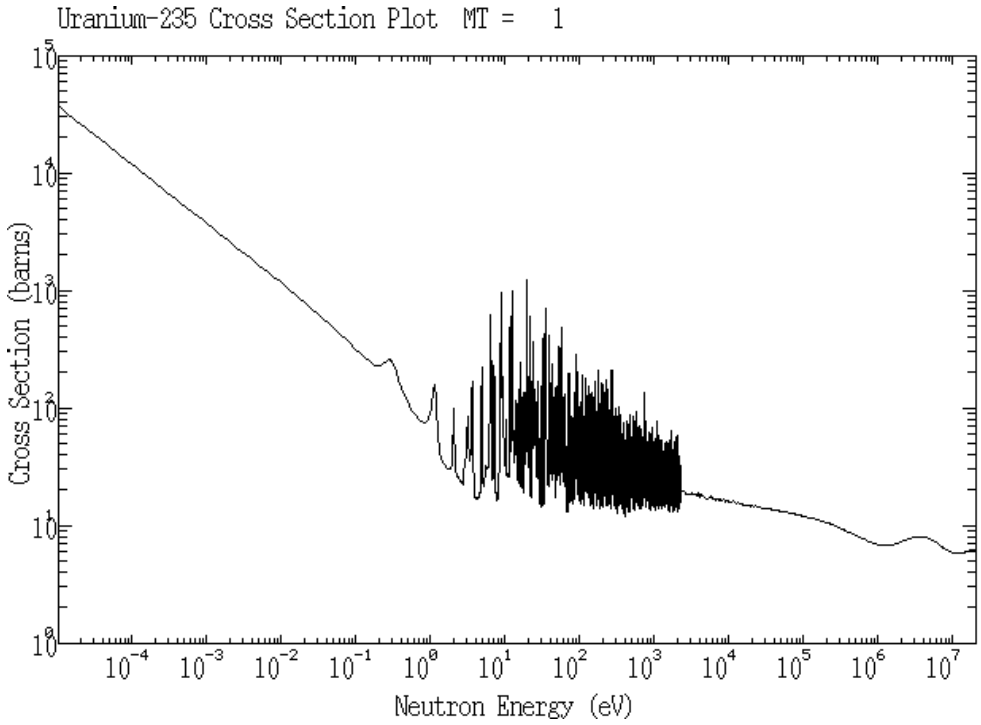

Figure B-3 Cross-section of U-235 vs. neutron energy[i]

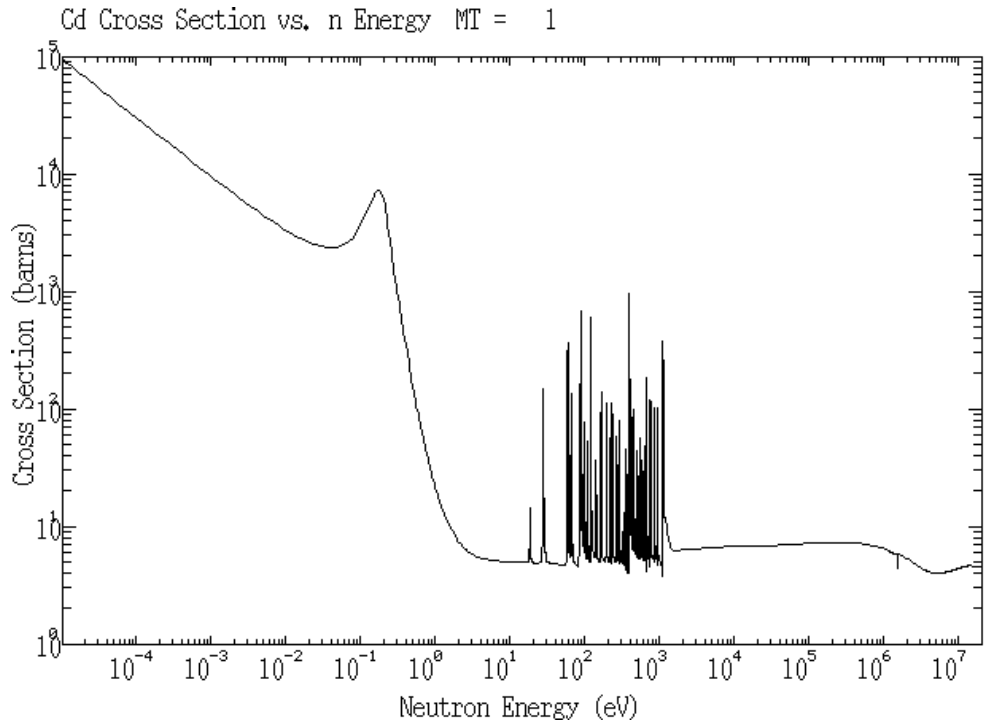

Figure B-4 Cross-section of Cd vs. neutron energy[i]

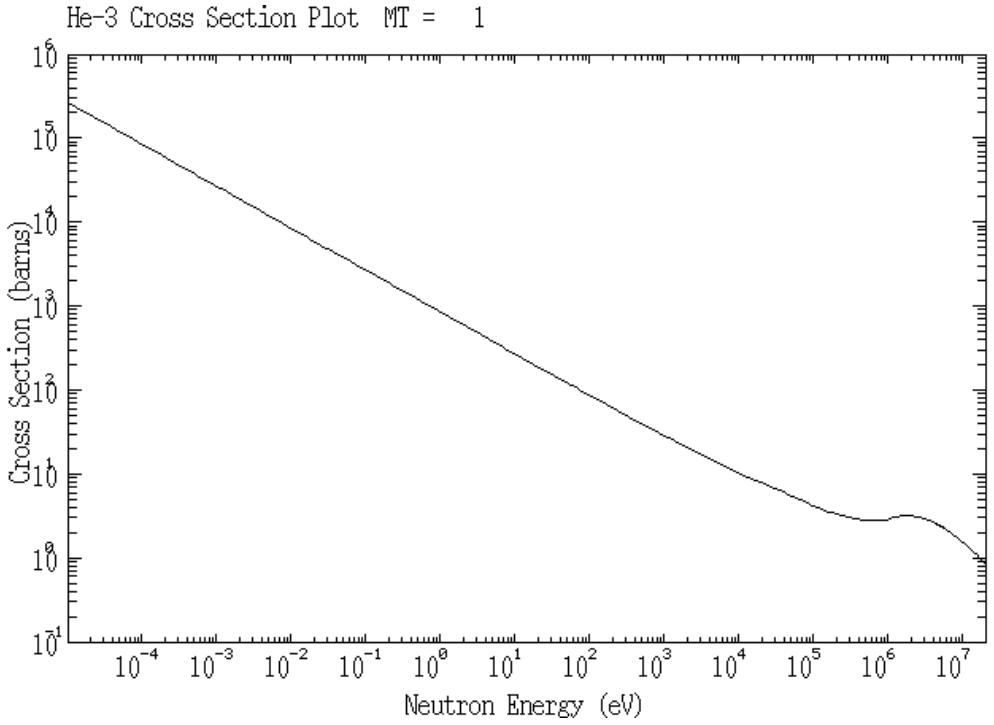

Figure B-5 Cross-section of He-3 vs. neutron energy[i]

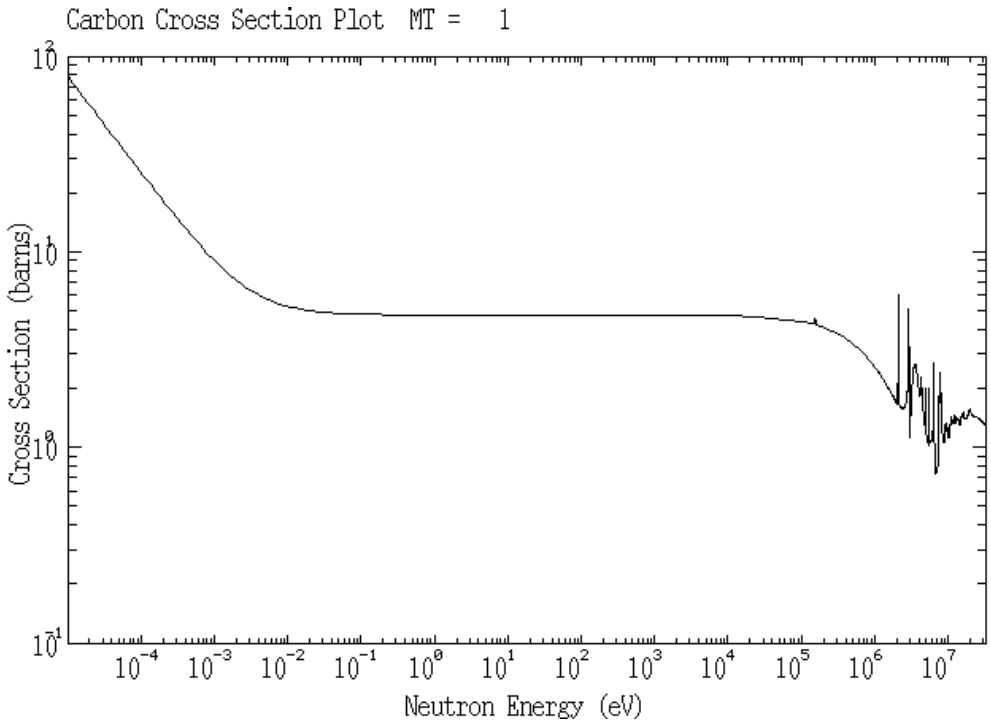

Figure B-6 Cross-section of Carbon vs. neutron energy[i]

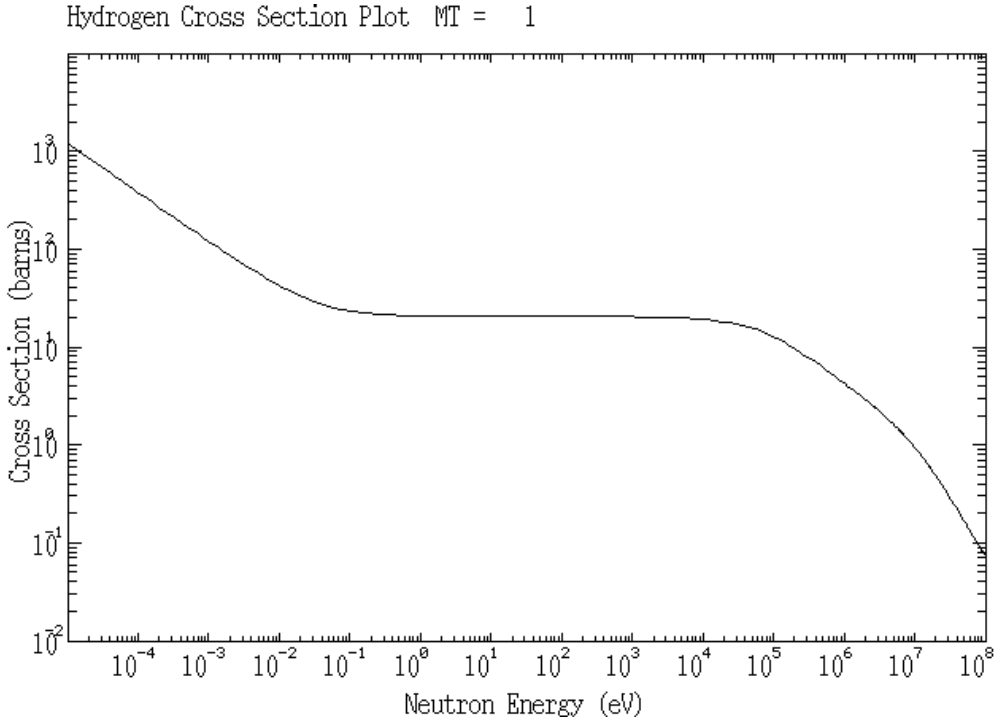

Figure B-7 Cross-section of Hydrogen vs. neutron energy[i]

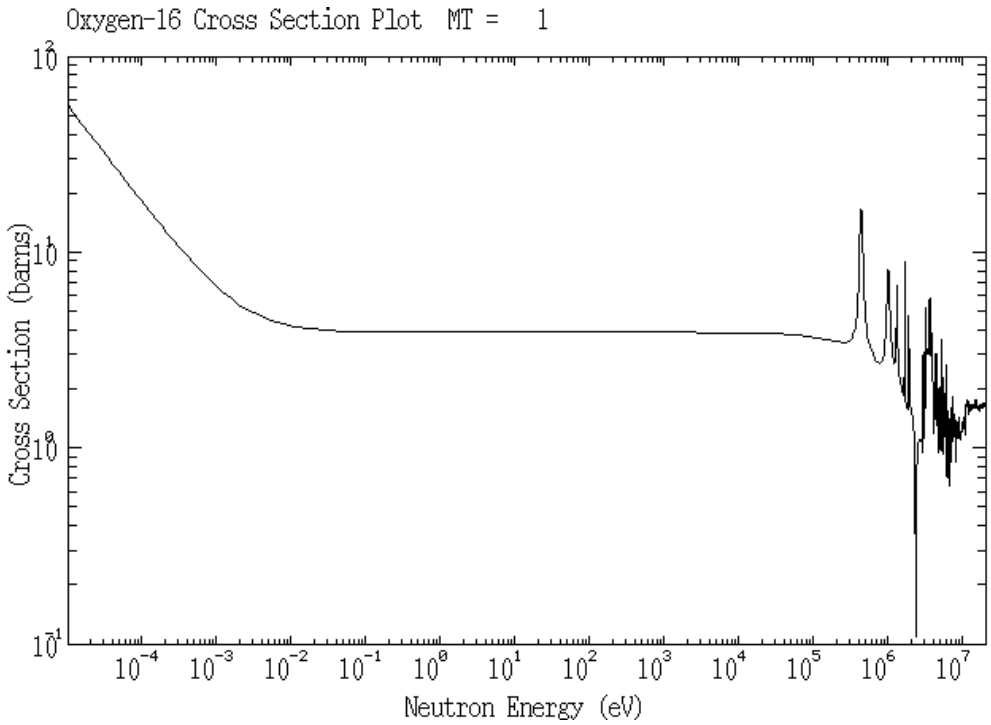

Figure B-8 Cross-section of Oxygen vs. neutron energy[i]

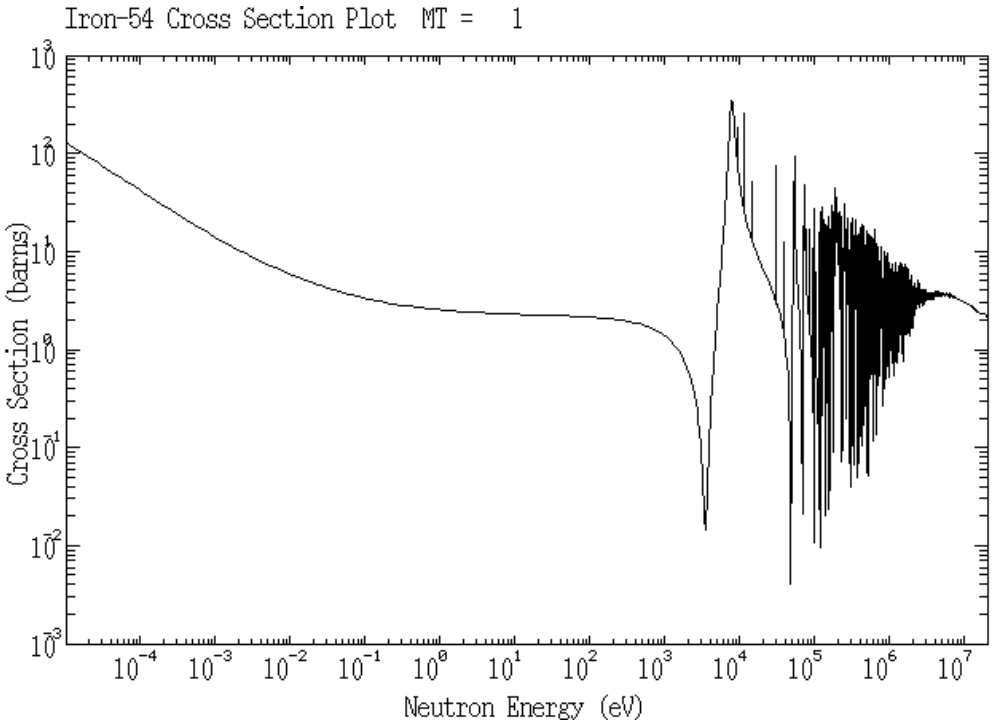

Figure B-9 Cross-section of Iron-54 vs. neutron energy[i]

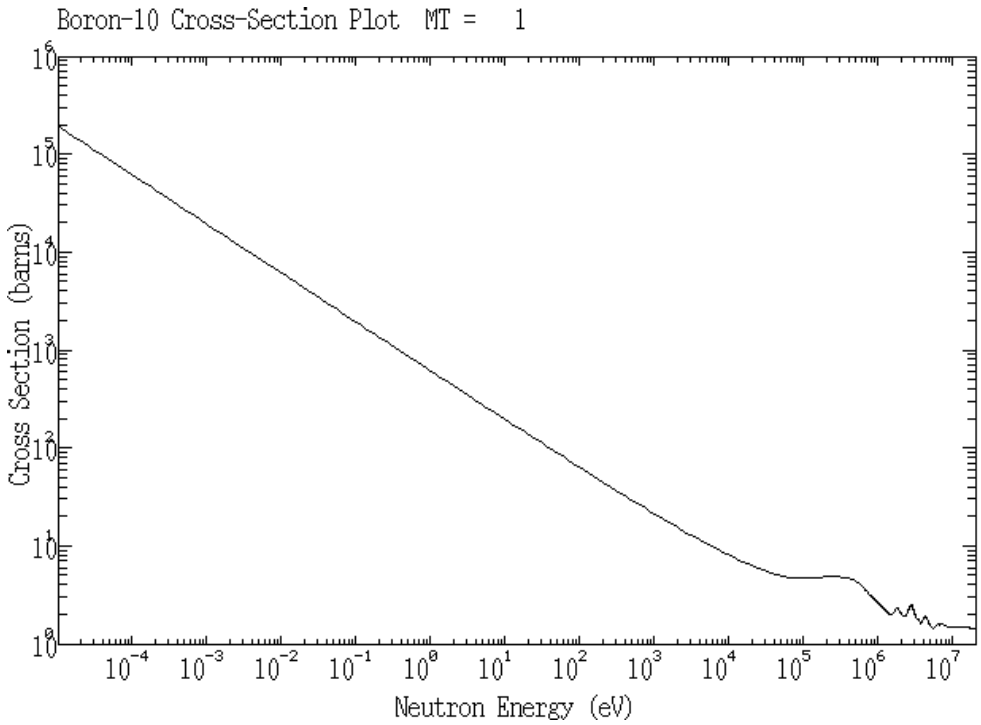

Figure B-10 Cross-section of B-10 vs. neutron energy[i]

[i] All cross section plots generated at http://hpngp01.kaeri.re.kr/CoN/endfplot.shtml
Courtesy of the Korean Atomic Energy Research Institute